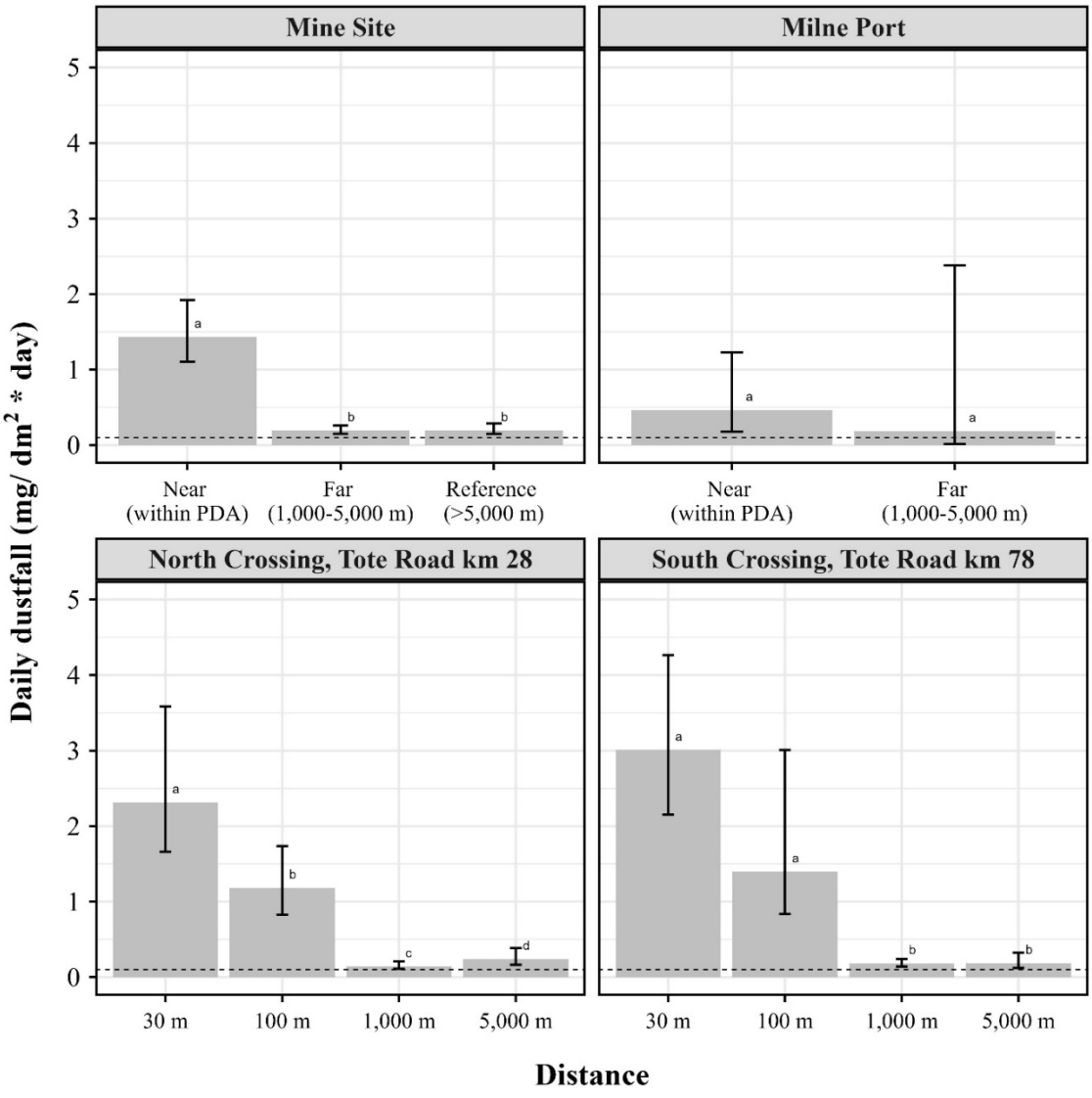

Figure 7-1. Geometric mean daily dustfall (mg/dm²·day) for the Mine Site, Milne Port, the Tote Road north crossing (KM 28), and the Tote Road south crossing (KM 78). The Tote Road sites are measured as a function of distance from the Tote Road. Scales are equal for each area to allow comparison of differences between each area.

Bar heights show geometric mean daily dustfall with 95% confidence intervals. Confidence intervals are asymmetrical because dust data were analyzed on the log$_e$ scale and back-transformed to the natural scale. The dashed horizontal line indicates the minimum detection limit for dust samples and the maximum dustfall rate at Reference sites unaffected by the Project.

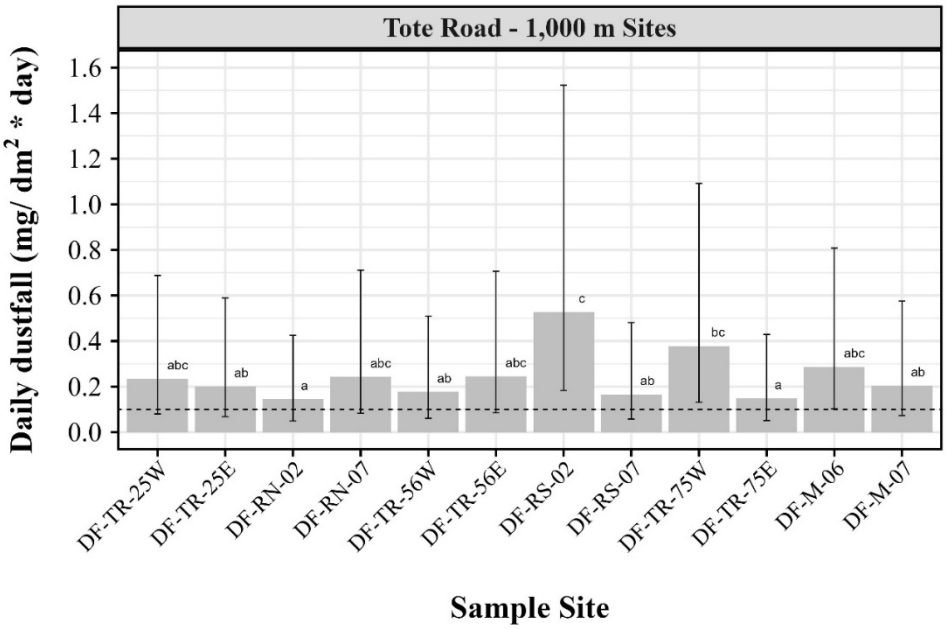

Figure 7-2. Geometric mean daily dustfall (mg/dm²·day) for all sites located 1,000 m from Project infrastructure during the summer season.

Bar heights show geometric mean daily dustfall with 95% confidence intervals. Confidence intervals are asymmetrical because dust data were analyzed on the log$_e$ scale and back-transformed to the natural scale. The dashed horizontal line indicates the minimum detection limit for dust samples and the maximum dustfall rate at Reference sites unaffected by the Project.

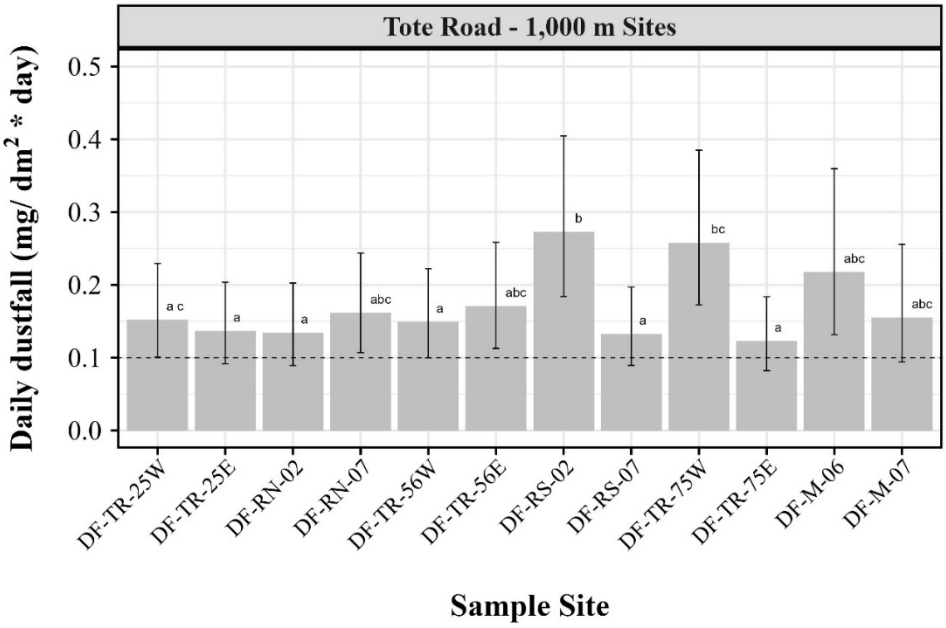

Figure 7-3. Geometric mean daily dustfall (mg/dm²·day) for all sites located 1,000 m from the Tote Road using year-round data.

Bar heights show geometric mean daily dustfall with 95% confidence intervals. Confidence intervals are asymmetrical because dust data were analyzed on the log$_e$ scale and back-transformed to the natural scale. The dashed horizontal line indicates the minimum detection limit for dust samples and the maximum dustfall rate at Reference sites unaffected by the Project.

7.3.2.2 Seasonal Comparisons of 2024 Dustfall

Seasonal variations in dustfall were investigated as per the dustfall monitoring objectives. Dustfall deposition across the PDA indicated different seasonal trends depending on location. Dustfall at the Mine Site was elevated during the winter (January through March) whereas dustfall at Milne Port was elevated in spring (May/June) and again in October. Dustfall along the Tote Road was elevated through spring and summer and lower during winter months when freezing conditions help to limit road-sourced dust. It has been noted for several years that spring and fall freeze/thaw conditions present challenges for dustfall mitigations such as road treatments (e.g., watering). Historically, elevated dustfall has been noted in September when variable freezing conditions may limit dust suppression; however, in September 2024 heavy rainfall closed the Tote Road for 17 days between September 8 and October 2.

Mine Site — Patterns across time were best represented by a common fluctuation in dustfall across months ($F1 = 3.54$, $P = 0.07$). Peaks occurred in April, July, and September/October (Figure 7-4). This model had a better trade off in complexity and variance explained relative to a model with month-only effects (AICc = 106.67 versus 113.39, respectively). The highest daily dustfall occurred in March (3.63 [95% CI = 1.53–7.00] mg/dm²·day) and the lowest daily dustfall occurred in September (0.41 [95% CI = 0.19–0.87] mg/dm²·day).

Milne Port — Patterns across time were best represented by mean differences among sites ($F4 = 35.55$, $P < 0.0001$) and months ($F11 = 12.45$, $P < 0.0001$). The peak in daily dustfall occurred in April (Figure 7-4). This model had a better trade off in complexity and variance explained relative to a model with month-only effects (AICc = 110.42 versus 181.46, respectively). The highest daily dustfall occurred in April at site DF-P-05 (3.96 [95% CI = 2.61–6.00] mg/dm²·day) and the lowest daily dustfall occurred in November at site DF-P-07 (0.09 [95% CI = 0.06–0.14] mg/dm²·day).

North Crossing, Tote Road KM 28 — Patterns across time were best represented by differences in sites ($\chi^2 3 = 8.47$, $P = 0.0003$) and month ($\chi^2 11 = 42.44$, $P < 0.0001$) (Figure 7-5). This model was the most parsimonious (AICc = 75.37) compared to models with an effect of season (ΔAICc = 21.15; Figure 7-6) or fluctuations across time (ΔAICc = 46.31; Figure 7-4). Geometric mean daily dustfall was highest at sites DF-RN-05 (15.64 [95% CI = 12.47–24.29] mg/dm²·day) and DF-RN-04 (12.96 [95% CI = 9.07–16.31] mg/dm²·day) in May 2024. Geometric mean daily dustfall was lowest at sites DF-RN-03 (0.26 [95% CI = 0.17–0.34] mg/dm²·day) and DF-RN-06 (0.34 [95% CI = 0.26–0.54] mg/dm²·day) in September 2024.

South Crossing, Tote Road KM 78 — Patterns across time were best represented by differences in sites ($F3 = 78.50$, $P < 0.0001$) and months ($F11 = 74.57$, $P < 0.0001$) (Figure 7-5). This model was the most parsimonious (AICc = 56.98) compared to models with an effect of season (ΔAICc = 31.32; Figure 7-5) or fluctuations across time (ΔAICc = 31.01; Figure 7-4). Geometric mean daily dustfall was highest at sites DF-RS-04 (31.39 [95% CI = 23.60–41.75] mg/dm²·day) and DF-RS-05 (23.34 [95% CI = 17.56–31.02] mg/dm²·day) in May 2024. Geometric mean daily dustfall was lowest at sites DF-RS-06 (0.29 [95% CI = 0.22–0.38] mg/dm²·day) and DF-RS-03 (0.35 [95% CI = 0.26–0.46] mg/dm²·day) in December 2024.

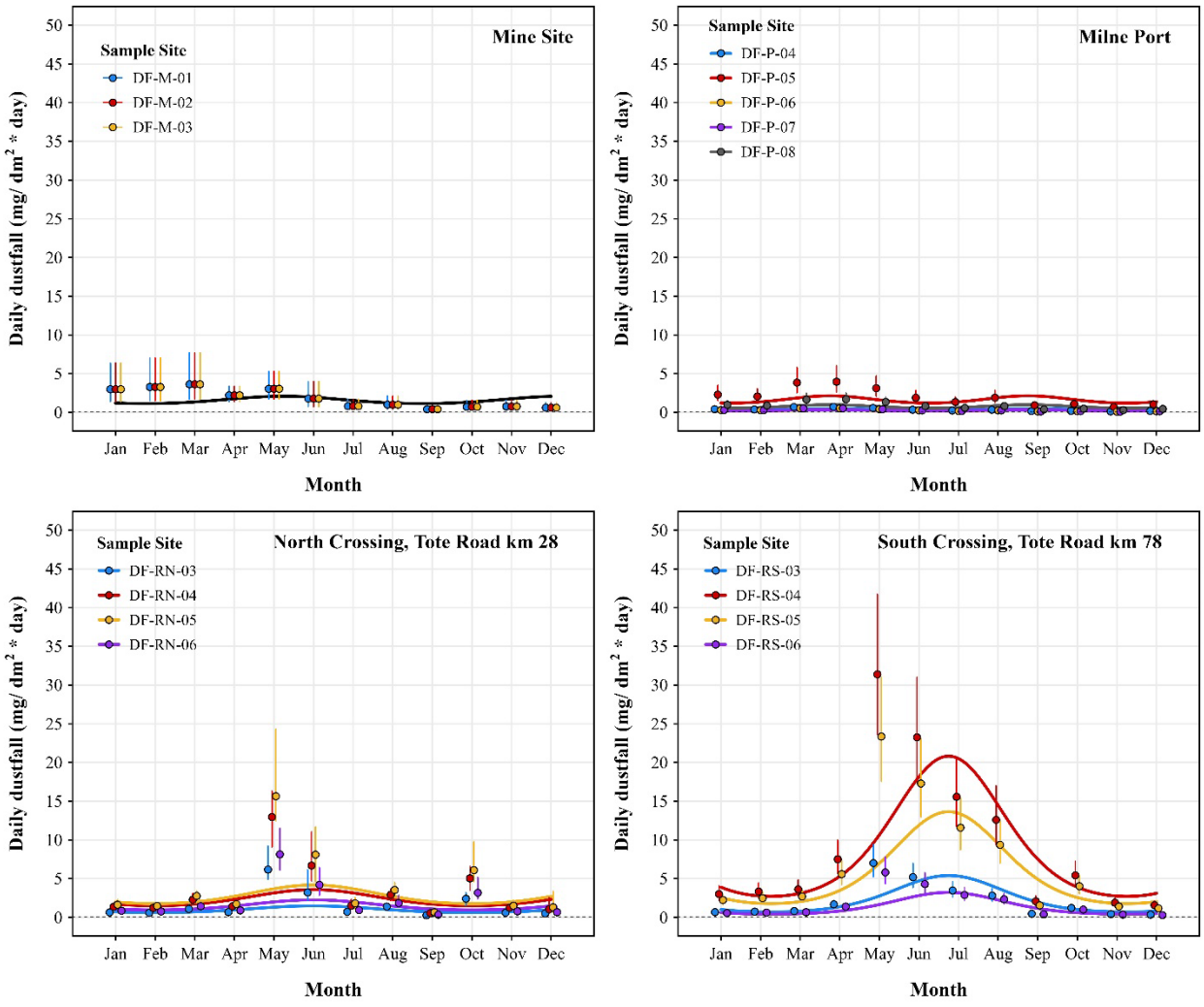

Figure 7-4. Geometric mean daily dustfall (mg/dm²·day) by site and month (time-series or category) or season (category) for the Mine Site, Milne Port, the Tote Road north crossing (KM 28), and the Tote Road south crossing (KM 78).

Bar heights show geometric mean daily dustfall with 95% confidence intervals. Confidence intervals are asymmetrical because dust data were analyzed on the $\log_e$ scale and back-transformed to the natural scale. Lines correspond with sinusoidal functions relative to each sample site. The dashed horizontal line indicates the minimum detection limit for dust samples and the maximum dustfall rate at Reference sites unaffected by the Project.

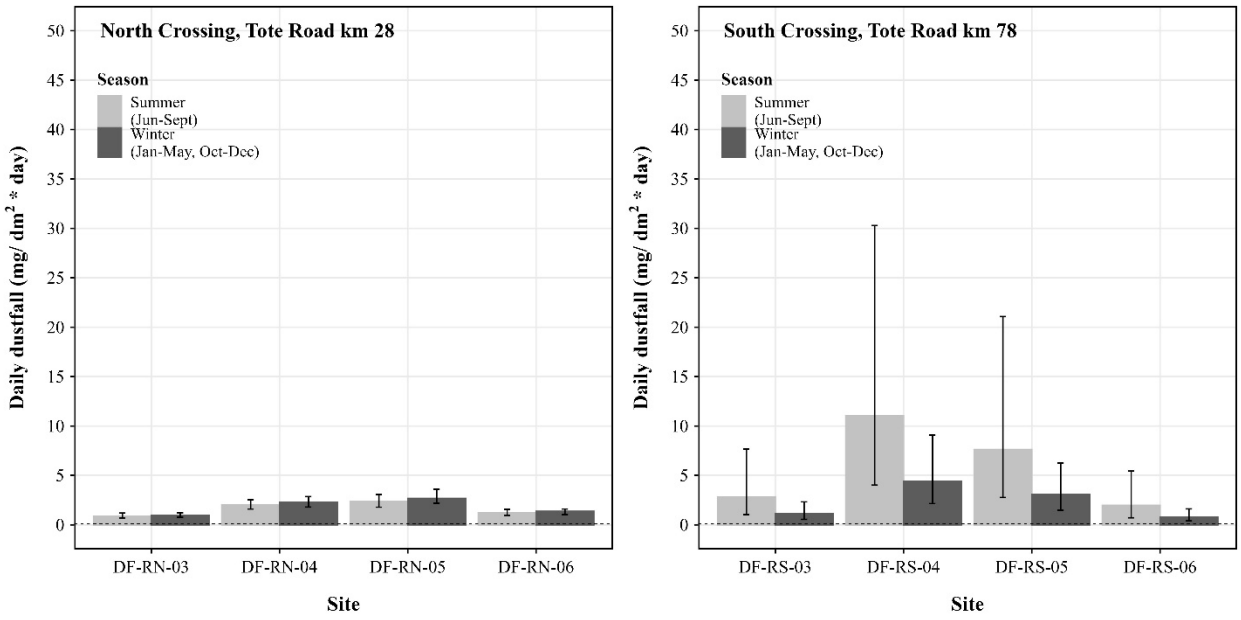

Figure 7-5. Geometric mean daily dustfall (mg/dm²·day) by site and season (summer and winter) for the Tote Road north (KM 28) and south (KM 78) crossings.

Bar heights show geometric mean daily dustfall with 95% confidence intervals. Confidence intervals are asymmetrical because dust data were analyzed on the log$_e$ scale and back-transformed to the natural scale. The dashed horizontal line indicates the minimum detection limit for dust samples and the maximum dustfall rate at Reference sites unaffected by the Project.

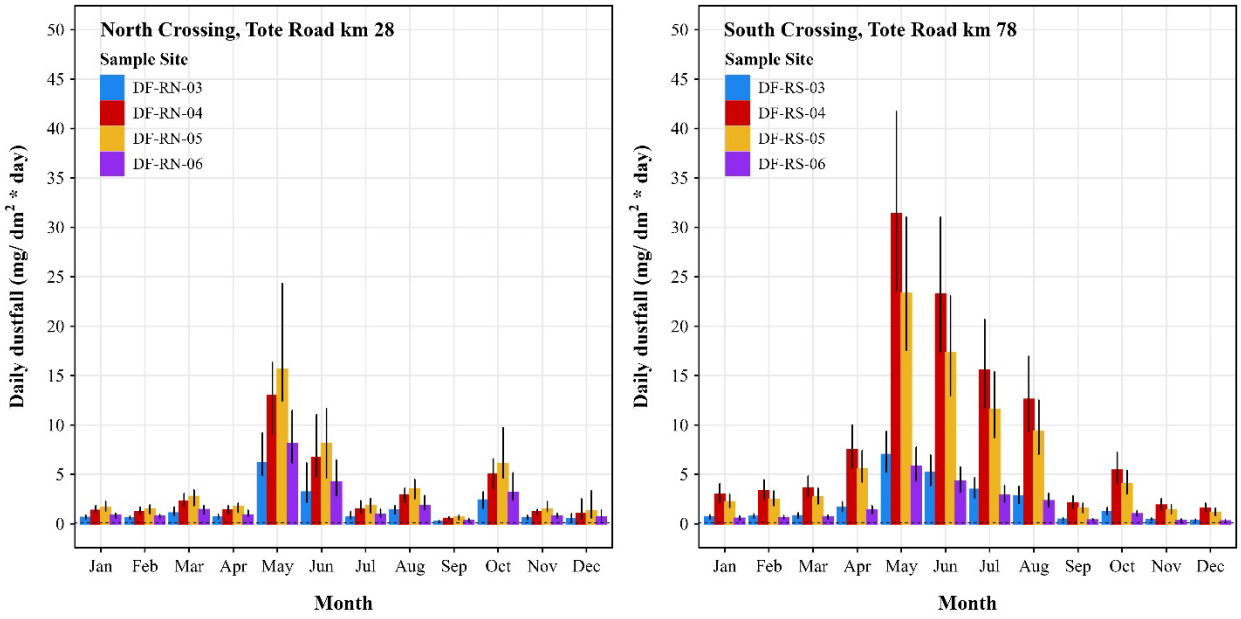

Figure 7-6. Geometric mean daily dustfall (mg/dm²·day) by site and month for the Tote Road north (KM 28) and south (KM 78) crossings.

Bar heights show geometric mean daily dustfall with 95% confidence intervals. Confidence intervals are asymmetrical because dust data were analyzed on the log$_e$ scale and back-transformed to the natural scale. The dashed horizontal line indicates the minimum detection limit for dust samples and the maximum dustfall rate at Reference sites unaffected by the Project.

7.3.2.3 2024 Annual Dustfall

Total annual dustfall for 2024 was calculated for all sites and each area in the Project RSA (Table 7-5, Figure 7-7, Figure 7-8). Annual dustfall quantities were based on those observed during monitoring and included predicted amounts (*) for sites that were sampled partially during the year (i.e., less than 365 days). For the latter sites, the total observed dustfall quantity was summed with the predicted dustfall during winter months when sampling did not occur. Those predictions were based on a model-based approach that estimated the quantity of dustfall during winter at sites at various distances from the Mine Site, Milne Inlet Port, and the Tote Road. The predicted quantities that were added to observed quantities of dustfall depended on the temporal coverage of each site during 2024. The following equation was used to calculate annual dustfall (g/m²/year) in Table 7-5:

$$Annual.Dust_{Total} = Annual.Dust_{Observed} + (Daily.Dust_{Predicted} \times [365 - Days.Sampled])$$

Table 7-5. Annual dustfall accumulation for sites sampled throughout 2024.[1]

Site	Area	Distance from PDA (km)	Model-predicted Annual Dustfall (g/m²/year)	Measured Annual Dustfall (g/m²/year)	Difference Between Predicted and Measured Dustfall (g/m²/year)
DF-M-01	Mine Site	0.00	38.6	50.99	12.39
DF-M-02	Mine Site	0.00	356.0	74.62	-281.38
DF-M-03	Mine Site	0.00	19.5	85.60	66.1
DF-M-04	Mine Site	9.23	5.5	5.81*	0.31
DF-M-05	Mine Site	9.23	5.5	5.82*	0.32
DF-M-06	Mine Site	1.18	5.5	20.97*	15.47
DF-M-07	Mine Site	1.23	5.5	20.09*	14.59
DF-M-08	Mine Site	4.09	5.5	12.97*	7.47
DF-M-09	Mine Site	3.35	5.5	13.55*	8.05
DF-P-03	Milne Inlet Port	3.27	5.5	3.60*	-1.9
DF-P-04	Milne Inlet Port	0.00	21.3	16.72	-4.58
DF-P-05	Milne Inlet Port	0.00	524.0	79.96	-444.04
DF-P-06	Milne Inlet Port	0.00	69.4	10.58	-58.82
DF-P-07	Milne Inlet Port	0.00	497.5	10.12	-487.38
DF-P-08	Milne Inlet Port	0.08	25.9	34.89	8.99
DF-P-09	Milne Inlet Port	1.00	14.0	9.65*	-4.35
DF-P-10	Milne Inlet Port	0.00	55.0	32.69*	-22.31
DF-P-11	Milne Inlet Port	1.17	5.5	6.05*	0.55
DF-P-12	Milne Inlet Port	1.35	5.5	5.87*	0.37
DF-RS-01	Road South	6.02	-	4.43*	-
DF-RS-02	Road South	0.63	-	10.92*	-
DF-RS-03	Road South	0.07	-	88.70	-
DF-RS-04	Road South	0.00	-	311.93	-
DF-RS-05	Road South	0.00	-	225.95	-

Table 7-5. Annual dustfall accumulation for sites sampled throughout 2024.[1]

Site	Area	Distance from PDA (km)	Model-predicted Annual Dustfall (g/m²/year)	Measured Annual Dustfall (g/m²/year)	Difference Between Predicted and Measured Dustfall (g/m²/year)
DF-RS-06	Road South	0.00	-	64.88	-
DF-RS-07	Road South	0.95	-	5.72*	-
DF-RS-08	Road South	6.67	-	3.94*	-
DF-RN-01	Road North	4.54	5.5	5.61*	0.11
DF-RN-02	Road North	1.00	3.8	5.62*	1.82
DF-RN-03	Road North	0.07	122.4	49.36	-73.04
DF-RN-04	Road North	0.00	270.4	121.75	-148.65
DF-RN-05	Road North	0.01	138.4	138.88	0.48
DF-RN-06	Road North	0.09	63.1	68.64	5.54
DF-RN-07	Road North	0.98	2.9	8.19*	5.29
DF-RN-08	Road North	5.92	5.5	4.90*	-0.60
DF-RR-01	Tote Road	13.99	-	2.09*	-
DF-RR-02	Tote Road	14.00	-	2.07*	-
DF-TR-25E	Tote Road	1.19	2.3	5.74*	3.44
DF-TR-25W	Tote Road	1.01	6.5	8.15*	1.65
DF-TR-56E	Tote Road	0.90	-	8.53*	-
DF-TR-56W	Tote Road	1.14	-	7.73*	-
DF-TR-75E	Tote Road	1.00	-	6.81*	-
DF-TR-75W	Tote Road	1.07	-	10.75*	-

[1] Annual accumulations are reported for the period January 23, 2024, to December 22, 2024.

* Extrapolated (winter) dustfall predictions were added to the observed dustfall amount. The amount added to the observed quantity was inversely proportional to the number of sampling days (i.e., lower total sampling days resulted in greater amounts added to observed dustfall quantities).

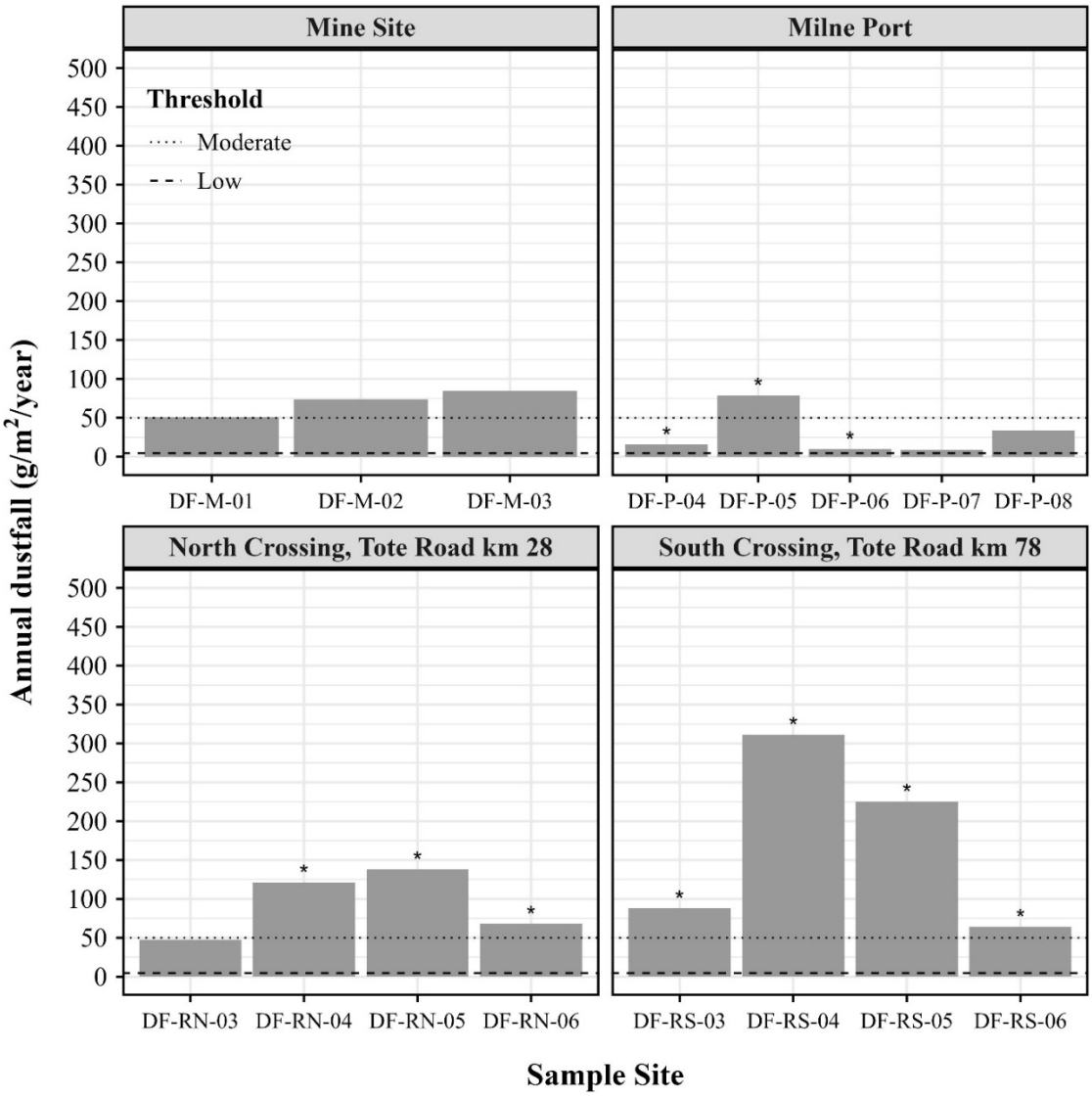

Figure 7-7. Annual dustfall (g/m²/year) for stations sampled year-round at the Mine Site, Milne Port, the Tote Road north crossing (KM 28), and the Tote Road south crossing (KM 78).
The dashed horizontal lines show low, moderate, and high dust isopleth upper limits. The asterisk (*) denotes that the annual dustfall was greater than projected by the predicted isopleth.

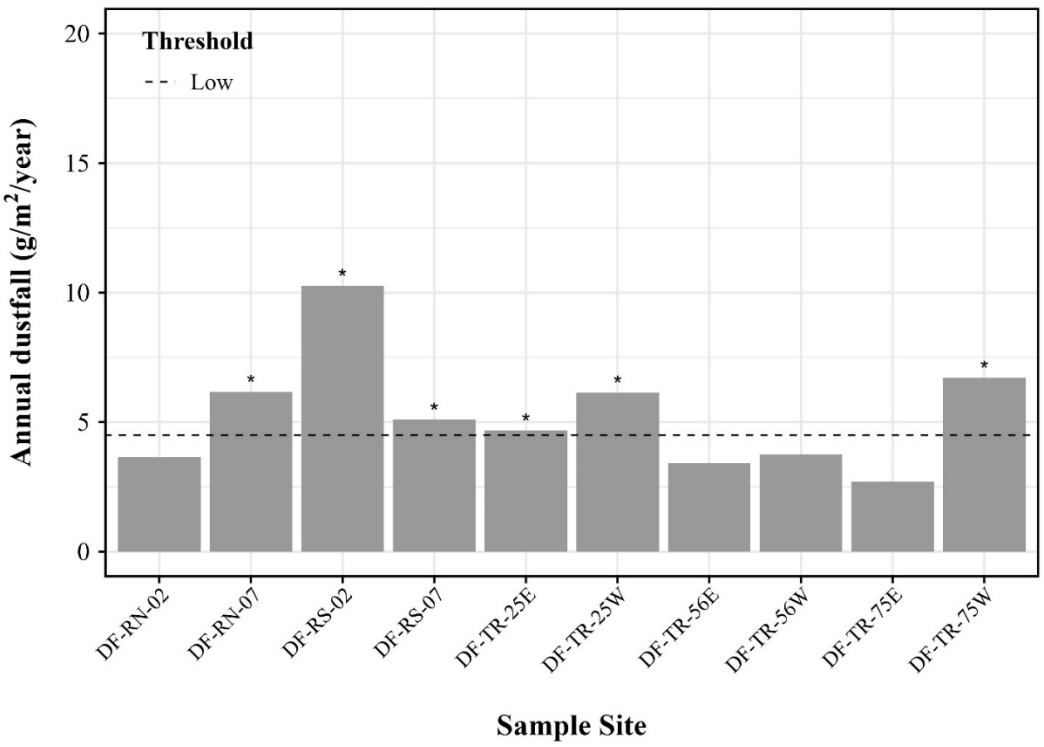

Figure 7-8. Total annual dustfall (g/m²/year) at the Tote Road sites located 1,000 m distance from the centreline.
The dashed horizontal line shows low dust isopleth upper limits. The asterisk (*) denotes that the annual dustfall was greater than projected by the predicted isopleth.

7.3.3 INTER-ANNUAL TRENDS

7.3.3.1 Seasonal Dustfall

Mine Site — Inter-annual patterns across time were best represented by differences in months (AIC_c = 1,024.58) rather than year-specific fluctuations (ΔAIC_c = 34.92) or a common fluctuation across time (ΔAIC_c = 19.22). The strongest evidence was for the effect of month (F_{11} = 6.78, P < 0.0001). Although an effect of year was evident (F_9 = 2.12, P = 0.03; Figure 7-9), greater statistical support was present for a month-only model over a model with both month and year effects (AIC_c = 1,024.58 versus 1,027.10, respectively). The greatest mean differences were between August versus March, April, and May (all P < 0.0001). Geometric mean daily dustfall rates were consistently highest in March, April, and May in each year. Among years, geometric mean daily dustfall rates were highest in 2016, 2021, and 2022 and lowest in 2015, 2019, and 2024 (Figure 7-9). Geometric mean daily dustfall rates in 2024 were lower than most years during peak months (i.e., 2.42 [95% CI = 1.02–5.75] mg/dm²·day in March to 2.73 [95% CI = 1.13–6.64] mg/dm²·day in May).

Milne Port — Sites DF-P-01 and DF-P-08 were removed from inter-annual dustfall analyses at Milne Port. Site DF-P-01 was located within 100 m of ore stockpiles from 2013 to 2019 and was decommissioned as a site in May 2019. Site DF-P-08 replaced DF-P-01 as a sample unit but was placed at distances >1,000 m from the PDA, which are expected to experience lower dust quantities than sites at the PDA. Therefore, both sites

were removed from analyses because inclusion of both would bias the inter-annual estimates of dustfall by erroneously indicating a sudden decrease in mean dustfall in 2020 and 2021. Inter-annual patterns were best represented by differences in months and years (AIC_c = 959.03) rather than year-specific fluctuations (ΔAIC_c = 14.39) or a common fluctuation across time (ΔAIC_c = 16.79). Both the month (F_{11} = 8.72, $P < 0.0001$) and year (F_9 = 3.95, $P < 0.0001$) effects were statistically significant. Geometric mean daily dustfall rates were consistently highest in April and October in each year. Among years, geometric mean daily dustfall rates were highest in 2016, 2019, and 2019 and lowest in 2015, 2021, and 2024 (Figure 7-10). Geometric mean daily dustfall rates in 2024 were lower than most years during peak months (i.e., 1.40 [95% CI = 0.24–8.16] mg/dm²·day in April and 0.91 [95% CI = 0.16–5.39] mg/dm²·day in October).

Tote Road — Dustfall along the Tote Road has been consistently elevated from April through October. This corresponds with early spring melt, summer, and early fall freeze-up. During the winter season when conditions are consistently frozen, dustfall is markedly less.

North Crossing, Tote Road KM 28 — Inter-annual patterns across time were best represented by differences in months and years (AIC_c = 1,090.72) rather than year-specific fluctuations (ΔAIC_c = 51.57) or a common fluctuation across time (ΔAIC_c = 65.09)[9]. Strong evidence for an effect of month (F_{11} = 64.78, $P < 0.0001$; Figure 7-11) and year (F_9 = 4.58, $P < 0.0001$) was present with a two-way analysis of variance (ANOVA), but normality and homoscedasticity assumptions were violated. Pairwise Wilcoxon tests revealed that the greatest differences in dustfall were between February and May, June, and July (all $P < 0.0001$). Geometric mean daily dustfall rates were consistently highest in June and July in each year. Among years, geometric mean daily dustfall rates were highest in 2015, 2020, and 2022 and lowest in 2016, 2018, and 2019 (Figure 7-11). Geometric mean daily dustfall rates in 2024 were lower than most years during peak months (i.e., 5.06 [95% CI = 4.18–6.11] mg/dm²·day in June and 4.28 [95% CI = 3.70–5.06] mg/dm²·day in July).

South Crossing, Tote Road KM 78 — Inter-annual patterns across time were best represented by differences in months and years (AIC_c = 1,127.43) rather than year-specific fluctuations (ΔAIC_c = 65.15) or a common fluctuation across time (ΔAIC_c = 93.69). Strong evidence for an effect of month (F_{11} = 107.56, $P < 0.0001$) and year (F_9 = 8.10, $P < 0.0001$) was present with a two-way ANOVA, but normality and homoscedasticity assumptions were violated. Pairwise Wilcoxon tests revealed that the greatest differences in dustfall were between June and January, February, November, and December (all $P < 0.0001$). Geometric mean daily dustfall rates were consistently highest in May, June, and July in every year. Among years, geometric mean daily dustfall rates were highest in 2020, 2022, and 2024 and lowest in 2016, 2017, and 2018 (Figure 7-12). Geometric mean daily dustfall rates in 2024 were higher than most years during peak months (i.e., 8.72 [95% CI = 7.31–10.62] mg/dm²·day in July to 11.84 [95% CI = 10.20–13.76] mg/dm²·day in June).

[9] Though year-specific fluctuations (interaction term) yielded a better overall fit than common fluctuations, model predictions for certain years were very inaccurate; thus, Figure 7-11 provides the common fluctuation (sinusoidal function).

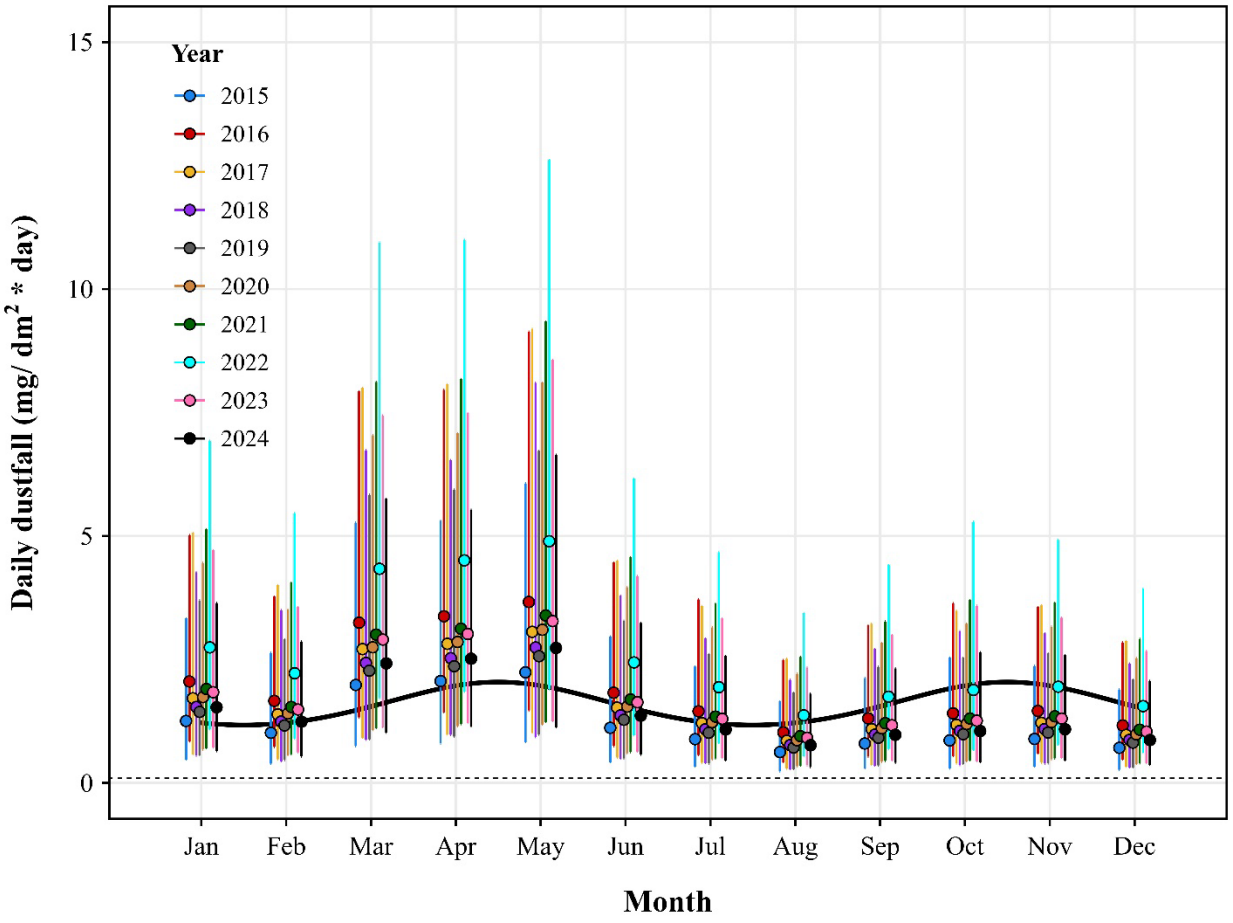

Figure 7-9. Inter-annual mean daily dustfall (mg/dm²·day) at the Mine Site (2015 to 2023).
Points show geometric mean daily dustfall with 95% confidence intervals. Confidence intervals are asymmetrical because dust data were analyzed on the log$_e$ scale and back-transformed to the natural scale. The dashed horizontal line indicates the minimum detection limit for dust samples and the maximum dustfall rate at Reference sites unaffected by the Project.

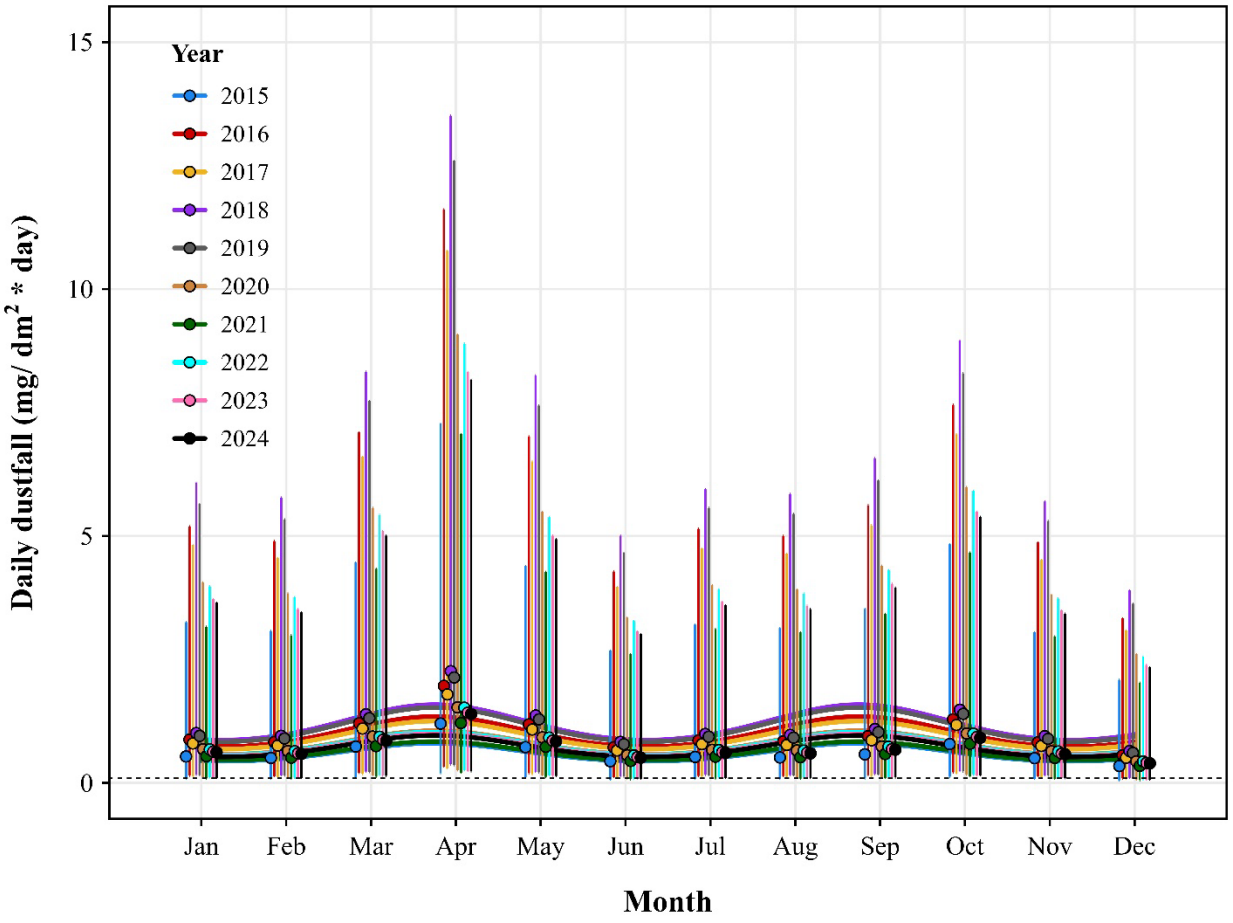

Figure 7-10. Inter-annual mean daily dustfall (mg/dm²·day) at Milne Port (2015 to 2023).
Points show geometric mean daily dustfall with 95% confidence intervals. Confidence intervals are asymmetrical because dust data were analyzed on the log$_e$ scale and back-transformed to the natural scale. Lines correspond with sinusoidal functions relative to each year. The dashed horizontal line indicates the minimum detection limit for dust samples and the maximum dustfall rate at Reference sites unaffected by the Project.

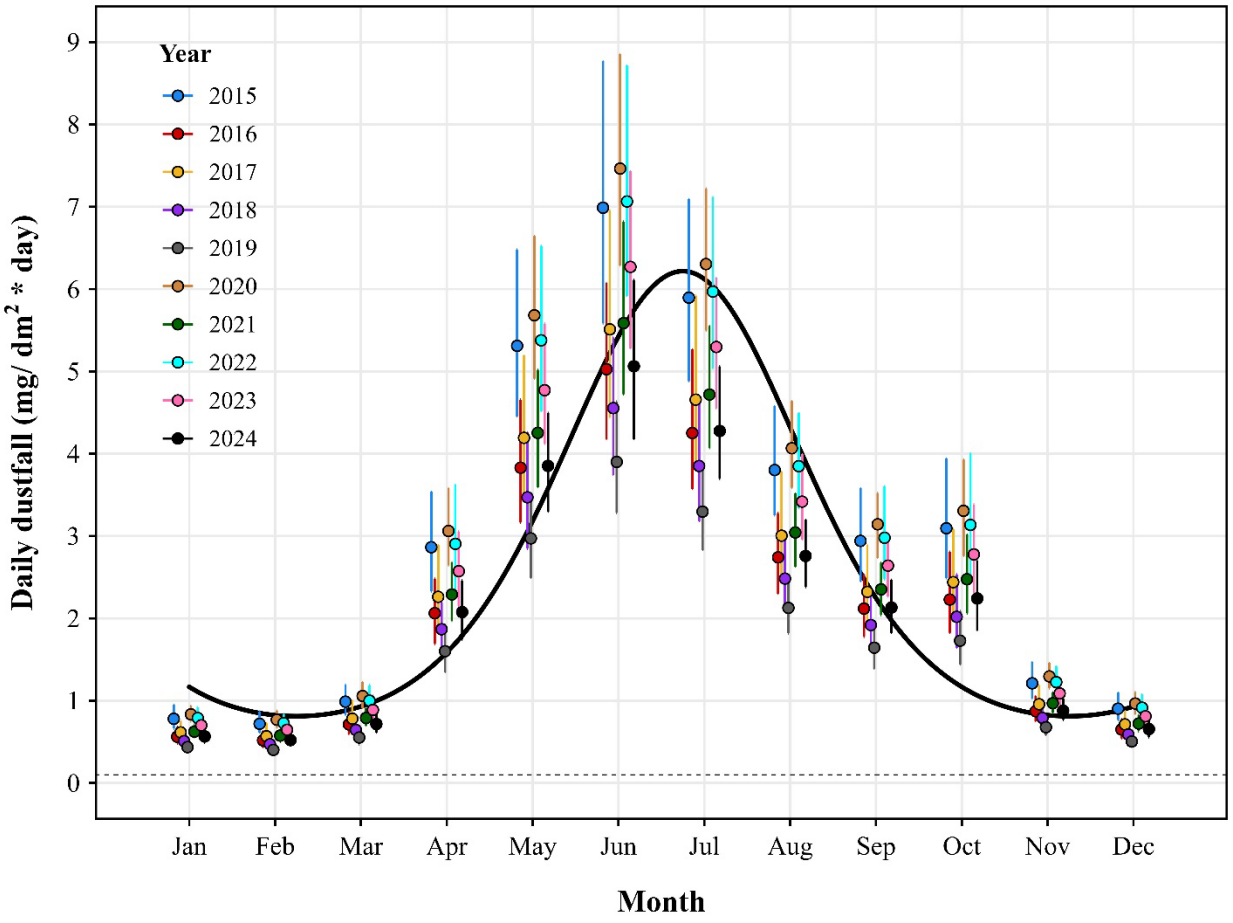

Figure 7-11. Inter-annual mean daily dustfall (mg/dm²·day) at the Tote Road north crossing (KM 28; 2015 to 2023).
Points show geometric mean daily dustfall with 95% confidence intervals. Confidence intervals are asymmetrical because dust data were analyzed on the log$_e$ scale and back-transformed to the natural scale. The dashed horizontal line indicates the minimum detection limit for dust samples and the maximum dustfall rate at Reference sites unaffected by the Project.

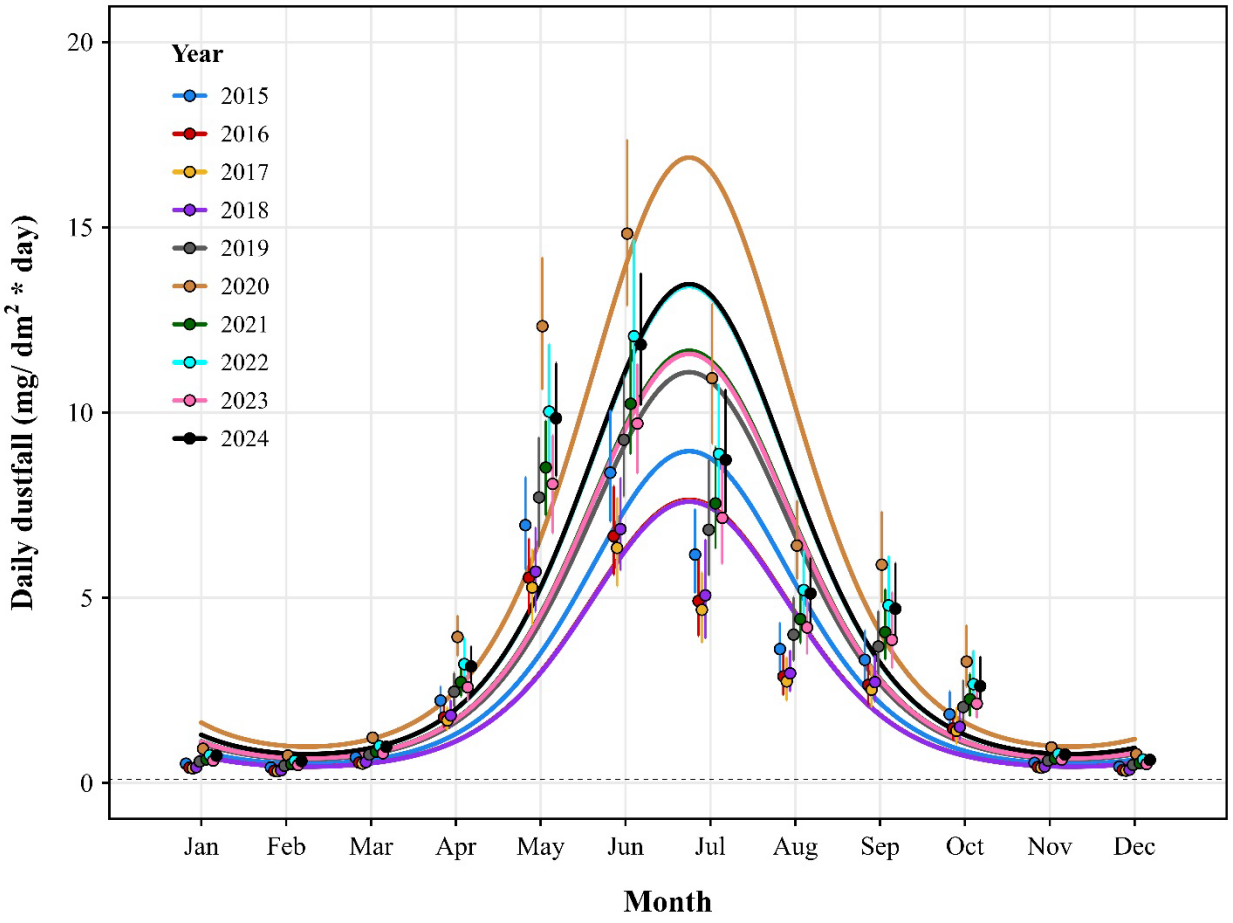

Figure 7-12. Inter-annual mean daily dustfall (mg/dm²·day) at the Tote Road south crossing (KM 78; 2015 to 2023).
Points show geometric mean daily dustfall with 95% confidence intervals. Confidence intervals are asymmetrical because dust data were analyzed on the log$_e$ scale and back-transformed to the natural scale. The dashed horizontal line indicates the minimum detection limit for dust samples and the maximum dustfall rate at Reference sites unaffected by the Project.

7.3.3.2 Total Annual Dustfall

From 2014 to 2016, dustfall across the PDA increased, corresponding with an increase in mine production. In 2016, production increased from 0.5 to 2.5 million tonne per annum, corresponding with increased dustfall; however, from 2016 to 2020, dustfall generally plateaued with only modest increases/decreases in some Project areas. Post-2016 decreases in dustfall appear to correspond with the implementation of additional dustfall mitigation strategies, though there continues to be some 'noise' that is believed to be associated with climate variations, specifically the number of days with measurable rainfall. Dustfall deposition in 2024 showed a generally decreasing trend across all Project areas.

Mine Site dustfall monitoring station DF-M-01 has recorded variable dustfall throughout all monitoring years. An increasing trend was observed from 2019 to 2021, followed by a decrease in 2022 and again in 2023 and 2024. Dustfall at DF-M-02 and DF-M-03 remained relatively consistent from 2018 to 2021, increased in 2022, and then decreased substantially in 2023, a trend that continued in 2024 (Figure 7-13).

Dustfall deposition at the Milne Port monitoring sites has remained relatively consistent since 2020. Dustfall at DF-P-05 decreased from 2018 to 2021 and increased slightly from 2022 to 2024. Dustfall has remained consistent at DF-P-04, DF-P-06, DF-P-07, and DF-P-08.

Dustfall along the Tote Road at the north crossing (KM 28) monitoring stations has remained relatively constant since 2019. Dustfall along the Tote Road at the south crossing (KM 78) monitoring stations 30 m from the road has been variable over the years but shows no consistent increasing or decreasing trends. Dustfall at the monitoring stations 100 m from the road has been consistent since 2015, the first full year of dustfall monitoring during mine operations. Dustfall at both crossing locations decreased from 2023 to 2024.

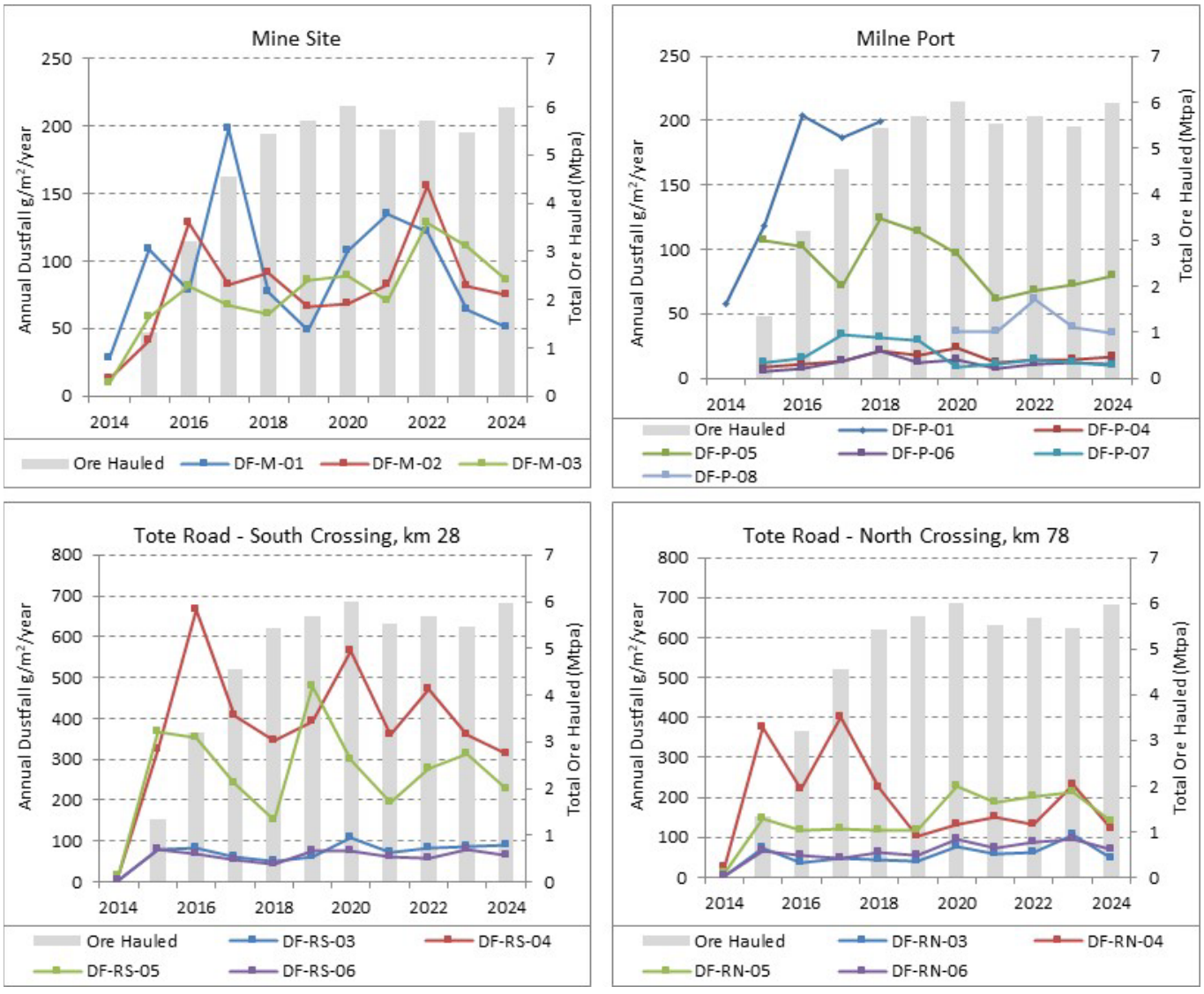

Figure 7-13. Year-over-year annual dustfall (g/m²/year) in relation to total ore mined and hauled to Milne Port.

7.4 DUSTFALL IMAGERY ANALYSIS

7.4.1 METHODS

Analysis of remotely sensed imagery was deemed appropriate and beneficial for estimating the spatial extents of dustfall at the Project, given (1) the high contrast and visibility of dust on the landscape[10] and (2) the detectability of dust using multispectral analysis. Dust and snow have different spectral characteristics affecting light absorption/reflection of different wavelengths. Multispectral bands (e.g., visible, near-infrared, and shortwave) of satellite imagery can differentiate dust and snow reflectance values, allowing for automated extraction of pixels representing dust coverage using comparisons of the various multispectral bands (i.e., band ratios).

7.4.1.1 Study Area

Dustfall imagery analysis has been used to estimate dustfall extent at the Project since 2020. The current Study Area (Map 7-2), developed in 2022, includes the 2008 RSA and identified Areas of Community Concern in the 2021 Dust Investigation report (Hutchinson Environmental Sciences Ltd. 2022). Areas of analysis include the PDA and 30 m, 100 m, 1 km, 5 km, and 20 km buffers. The buffers were divided into five component areas: Mine Site, Milne Port, the Tote Road north, the Tote Road south, and Milne Inlet, including the inlet up to the north end of Stephens Island (Map 7-2).

[10] At ground level, dust on the snow can be visible at dustfall deposition levels as low as 0.1 to 0.2 g/m² (Li et al. 2013).

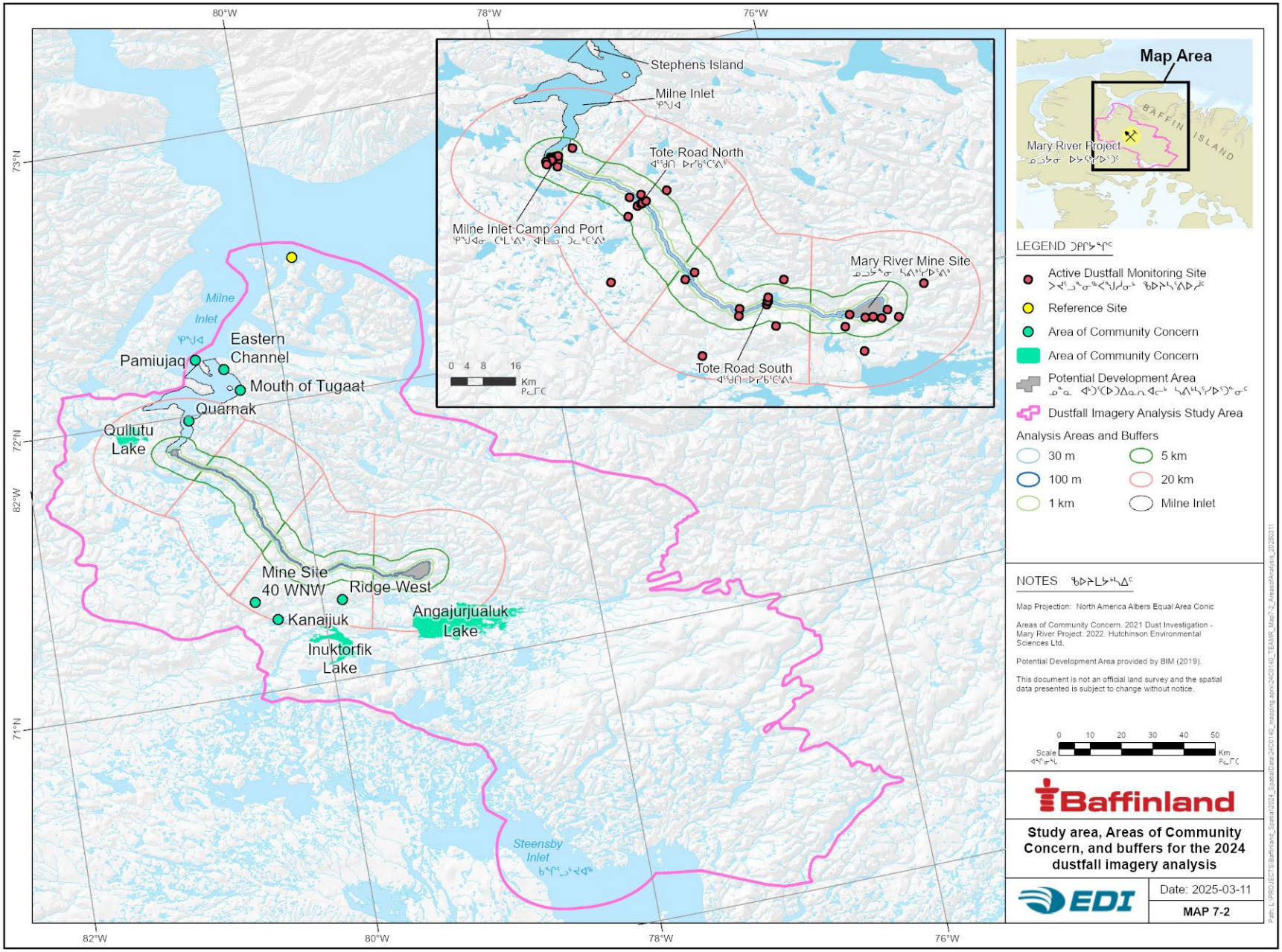
80°W
78°W
76°W
73°N
72°N
71°N
82°W
Stephens Island
Milne Inlet
ᖭᓐᔪᐊ
Tote Road North
ᐊᑦᓂᑎ ᐅᓪᓚᑦᑕᐃᓐ
Milne Inlet Camp and Port
ᖭᓐᔪᐊᓂᕐ ᑕᒪᓐᐃᓐ ᐊᒥᓚᓄ ᑐᓴᒃᑕᐃᓐ
Mary River Mine Site
ᓂᓪᓕᖅᓂ ᒪᓇᐱᓪᓕᐅᖅᐃᓐ
Tote Road South
ᐊᑦᓂᑎ ᐅᓪᓚᑦᑕᐃᓐ
0 4 8 16
Km
ᑭᓪᓕᒥ
Milne Inlet
ᖭᓐᔪᐊ
Eastern Channel
Pamiujaq
Mouth of Tugaat
Quarnak
Qullutu Lake
Mine Site 40 WNW
Ridge West
Kanajjuk
Angajurjualuk Lake
Inuktorfik Lake
Steensby Inlet
ᑲᖏᑦᓴᓕᐊᖅ
Map Area
Mary River Project
ᓂᓪᓕᖅᓂ ᐅᓴᖏᓪᓕᐅᑎᑦ
BAFFIN ISLAND
LEGEND ᑐᑭᓯᔾᔪᑦ
Active Dustfall Monitoring Site
Reference Site
Area of Community Concern
Area of Community Concern
Potential Development Area
Dustfall Imagery Analysis Study Area
Analysis Areas and Buffers
30 m
5 km
100 m
20 km
1 km
Milne Inlet
NOTES ᖃᐅᔨᓴᖅᓱᐃᓐᓇᑦ
Map Projection: North America Albers Equal Area Conic
Areas of Community Concern. 2021 Dust Investigation - Mary River Project. 2022. Hutchinson Environmental Sciences Ltd.
Potential Development Area provided by BIM (2019).
This document is not an official land survey and the spatial data presented is subject to change without notice.
0 10 20 30 40 50
Scale
Km
ᑭᓪᓕᒥ
Baffinland
Study area, Areas of Community Concern, and buffers for the 2024 dustfall imagery analysis
EDI
Date: 2025-03-11
MAP 7-2

7.4.1.2 Imagery Acquisition

Imagery from Landsat 8 Operational Land Imager (OLI), Landsat 9 Operational Land Imager-2 (OLI-2), and Sentinel-2 Multispectral Instrument (MSI) sensors were used in the dustfall imagery analysis (Table 7-6). Landsat data are available from the United States Geological Survey and have a revisit time of eight days with the combined satellites (US Geological Survey 2022). Sentinel-2 data are available from the European Space Agency and have a revisit time of five days (European Space Agency 2020a). Images between March 15 and May 15, 2024, were selected for the dustfall imagery analysis. This period was chosen for extensive snow cover and available light. Where available, multiple images covering the same area were chosen to account for dustfall extent variability due to snowfall events that regularly bury dust and snowmelt that can cause dust to accumulate on the snow surface (Li et al. 2013).

Surface reflectance products were downloaded from the United States Geological Survey EarthExplorer website (US Geological Survey 2024) and the Copernicus Open Access Hub (European Space Agency 2024). The surface reflectance product contains georeferenced images corrected for topography and atmospheric conditions, giving reflectance values for each pixel as they appear at the Earth's surface (European Space Agency 2020b, Jenkerson 2023). Landsat images came with pixel quality masks identifying pixels representing clouds, cloud shadows, snow, and saturated pixels. Sentinel-2 images came with a classification mask, including categories for saturated/defective pixels, clouds and cloud shadows, water, vegetation, non-vegetated areas, and snow.

Table 7-6. Summary of satellite imagery used for dustfall extent imagery analysis.

Mission	Analysis Years	Sensor	Image Tiles	Bands[1]	Resolution
Landsat 5	2004–2011 (baseline)	Thematic Mapper (TM)	26-11, 27-10, 27-11, 28-10, 28-11, 29-10, 30-09, 30-10, 31-09, 31-10, 32-09, 32-10, 33-09 and 34-09	Band 2: G 0.52–0.60 µm Band 3: R 0.63–0.69 µm	30 m 30 m
Landsat 8	2013 (baseline) 2014–2024	Operational Land Imager (OLI)	26-11, 27-10, 27-11, 28-10, 28-11, 29-10, 30-09, 30-10, 31-09, 31-10, 32-09, 32-10, 33-09 and 34-09	Band 3: G 0.53–0.59 µm Band 4: R 0.64–0.67 µm	30 m 30 m
Landsat 9	2022–2024	Operational Land Imager-2 (OLI-2)	26-11, 27-10, 27-11, 28-10, 28-11, 29-10, 30-09, 30-10, 31-09, 31-10, 32-09, 32-10, 33-09 and 34-09	Band 3: G 0.53–0.59 µm Band 4: R 0.64–0.67 µm	30 m 30 m
Sentinel-2	2019–2024	Multispectral Instrument (MSI)	16WFE, 16XFF, 17WMV, 17WNT, 17WNU, 17WNV, 17WPT, 17WPU, 17WPV, 17XMA, 17XNA, 18WVC, 18WVD, and 18WVE	Band 3: G 0.54–0.58 µm Band 4: R 0.65–0.68 µm	20 m 20 m

[1] G = Green and R = Red.

7.4.1.3 Image Preprocessing

R version 4.2.2 (R Development Core Team 2023) and ArcGIS Pro 3.4 (ESRI 2024) were used to process and analyze the images. Saturated pixels were excluded from the analysis using the provided masks. Saturated pixels occur when the high reflectance of the surface (e.g., fresh snow) is beyond the sensor's range, causing sensor saturation. For Landsat images, saturated pixel masks were derived from the radiation saturation quality band and cloud masks were generated from the pixel quality band. For Sentinel-2 images, the provided classification masks were used to remove all pixels not classified as snow. Cloud masks were generally not adequate to remove clouds. A visual check was conducted to remove images with identifiable clouds (i.e., images that could skew data analysis). Sentinel-2 images with a zenith angle >70° were also excluded from analysis as recommended in the technical guide (Louis and L2A Team 2021).

The surface reflectance values of the red and green bands were also corrected for topographic illumination. The terrain correction was based on an illumination angle raster derived from the sun's position, slope, and aspect (Civco 1989, Colby 1991, Hantson and Chuvieco 2011) and was used in the C-correction method (Teillet et al. 1982, Hantson and Chuvieco 2011) to create a new raster for the red and green bands with topographically corrected reflectance values (EDI Environmental Dynamics Inc. 2024). The resulting image database represented high-quality satellite images within the Study Area from mid-March to mid-May for 2024, when dust should be detectable against a snow-covered landscape with minimal spectral or atmospheric interference.

7.4.1.4 Image Analysis

The 2024 dustfall imagery analysis focused on identifying, extracting, and quantifying mineral dust produced from mining activities at the Project. The image bands used for the analysis represent ranges of wavelengths on the electromagnetic spectrum. Features such as snow, rock, and vegetation absorb and reflect at different wavelengths. These distinct absorption and reflection characteristics can be used to identify and extract features from the imagery using combinations of bands. The SDI, (red−green)/(red+green), was used in the analysis as it was explicitly created to extract mineral dust on snow from imagery and can provide a relative estimation of mineral dust magnitude (Mauro et al. 2015). The SDI values ranged from -1 to 1, with positive values representing dust.

An SDI layer was calculated for each image from the original red and green bands and the terrain-corrected red and green bands. A mask of waterbodies and flat areas was created to combine the two SDI layers because flat areas do not require terrain correction. The resulting single SDI layer used the original SDI values within the mask and the terrain-corrected SDI values for all other areas.

7.4.1.5 Dustfall Extent and Magnitude

Satellite-derived dustfall concentration was estimated from the relationship between dustfall accumulation calculated from the dustfall deposition rates measured by the passive dustfall monitors and the SDI values from the imagery analysis. For each satellite image, a period of dustfall was determined, where the start date was the last snowfall event, and the end date was the date of the image. Snowfall events were determined from

daily recorded weather observations (2022 to 2024) or as days where precipitation was measured at the Mine Site or Milne Port weather stations, and the temperature was below freezing (2014 to 2021). Dustfall accumulation (g/m²) was calculated as the sum of the daily dustfall over each image period. Snow Darkening Index values were extracted from each image at dustfall monitor sites (Map 7-2) and compared with the calculated dustfall accumulation.

Landsat and Sentinel-2 images were processed separately because the SDI values between the two image datasets were determined to be significantly different (mean difference = 0.0099 [CIs = 0.0096–0.0102]; t2161 = 57.65, P <0.0001) in the 2022 Terrestrial Environment Annual Monitoring Report (EDI Environmental Dynamics Inc. 2023c). Linear regression models were developed for each dataset and applied to the individual SDI layers. The resulting dustfall concentration layers from all images (Sentinel-2 and Landsat) were combined into a 2024 composite dataset, taking the maximum concentration at each pixel. The 2024 composite dataset represented the maximum dustfall extent and concentration within the Study Area between March 14 and May 16, 2024. Composite datasets were also recreated for the pre-baseline (2004 to 2013) and post-baseline (2014 to 2023) years using the updated linear regression models that incorporated the 2024 data.. Composite datasets and subsequent analysis were conducted using the North American Albers Equal Area Conic spatial reference and a 30 m pixel size.

A baseline dustfall concentration layer was created from the mean concentration of the composite datasets from 2004 to 2011 and 2013, representing the mean background dust extent and concentration before construction of the Project. The baseline dataset was subtracted from the 2024 and previous post-baseline (2014 to 2023) dustfall concentration datasets to convey the spatial extent and estimated dustfall concentrations possibly produced by Project activities. To represent annual variability in the baseline dataset, dustfall concentration datasets were created for a high concentration and extent year (2004) and a low concentration and extent year (2013). The baseline dataset was subtracted from the high and low baseline years to allow for comparison with the post-baseline datasets.

Mean dustfall concentration was calculated within the PDA and the 30 m, 100 m, 1 km, 5 km, and 20 km buffers for the Mine Site, Milne Port, Milne Inlet, the Tote Road north, and the Tote Road south areas (Map 7-2). For the Areas of Community Concern, mean dustfall concentration was calculated within the lake boundaries or a 100 m buffer around a point feature to sample multiple pixels in the area.

Dustfall concentrations were classified into seven classes (i.e., <1, 1–4.5, 4.5–10, 10–20, 20–40, 40–50, and >50 g/m²) and analyzed for each component of the Study Area (i.e., Mine Site, Milne Port, Milne Inlet, the Tote Road north, and the Tote Road south). The area was calculated by multiplying the number of pixels within each class by the area of the pixel (i.e., 900 m² for a 30 m pixel resolution).

7.4.1.6 Snow Sampling Pilot Study

Calculated dustfall accumulation from the passive dustfall monitor deposition rates can estimate dustfall concentration to apply to the SDI values. This approach assumes no redistribution of dust after deposition and relies on estimating the period over which accumulation occurs. However, the SDI is a measure of the

magnitude of mineral dust concentration on the snow surface at the time of image acquisition, which is influenced by dust deposition and redistribution.

To investigate a potential method for estimating the dust concentration visible in the imagery, surface snow samples were collected based on the methods of Mauro et al. (2015). Improving on the surface snow sampling in 2022 and 2023, samples were collected in 2024 between May 20 and 29 on cloud-free days, using the dates and locations of satellite imagery acquisitions to guide efforts. The following procedures were conducted during field sampling to provide quality assurance and quality control (Baffinland Iron Mines Corporation 2022b):

- The 2.5 gallon high-density polyethylene pails used for sample collection were rinsed with deionized water three times.
- New nitrile gloves were worn during each sample collection and sample set collections.
- A 1.4 m x 1.4 m (2 m^2) square was measured on the snow surface, and the top 5 cm of the snowpack was transferred to a plastic pail using a plastic shovel.
- Samples were melted under cool conditions (≤4°C).
- Samples were stirred and agitated using a clean spatula.
- Bottles were rinsed three times with melt water before being filled, and a new syringe (no filter) was used for each site to fill the bottles.
- Field duplicates, field blanks, travel blanks, and equipment blanks were collected.

Sample bottles, duplicates, and blanks were sent to the ALS Environmental Laboratory in Waterloo, Ontario, to analyze Total Suspended Solids (units of mg/L) and a suite of metals. Only the Total Suspended Solids measurements were used for comparison with SDI values.

Snow Darkening Index values were extracted from Landsat and Sentinel-2 images acquired on the same date as the surface snow samples. A non-linear regression was created using R version 4.2.2 (R Development Core Team 2023) and the rational function from Mauro et al. (2015) for mineral dust versus SDI measured from hyperspectral data collected from a spectroradiometer.

$$f(x) = \frac{p_1 x + p_2}{x + q_1}$$

A range of starting values were used for p_1 (0.05 to 0.5), p_2(-10.5 to -0.5), and q_1(0 to 1,000) and the mean of the resulting coefficients was used as the final starting value for the model. Residual diagnostic plots were examined to confirm assumptions of normality and equality of variance in the residuals.

7.4.2 RESULTS AND DISCUSSION

7.4.2.1 Scene Distribution

Sixty-three suitable Sentinel-2 images were acquired over 18 unique dates in 2024, comparable to 2023 (Table 7-7). The number of suitable Landsat images decreased from 56 to 26 and were acquired over 18 unique dates in 2024. For 2024, Sentinel-2 images were distributed across the acquisition period, with late April having the lowest number (Figure 7-14A). The number of suitable Landsat images was highest in late March (Figure 7-14A). Both satellite image datasets had good spatial coverage and multiple images for all areas within the Study Area (Figure 7-14B).

Table 7-7. Remote sensing sources used for dustfall imagery analysis.

Satellite	Unique Counts	Baseline (2004 to 2013)	2014	2015	2016	2017	2018	2019	2020	2021	2022	2023	2024
Landsat 5	Dates	59	–	–	–	–	–	–	–	–	–	–	–
	Images	75	–	–	–	–	–	–	–	–	–	–	–
Landsat 8	Dates	10	14	18	12	8	10	9	17	11	9	19	10
	Images	12	19	25	15	15	16	11	26	16	12	28	14
Landsat 9	Dates	–	–	–	–	–	–	–	–	–	7	17	8
	Images	–	–	–	–	–	–	–	–	–	12	28	12
Sentinel-2	Dates	–	–	–	–	–	–	8	29	2	9	16	18
	Images	–	–	–	–	–	–	28	106	13	37	67	63

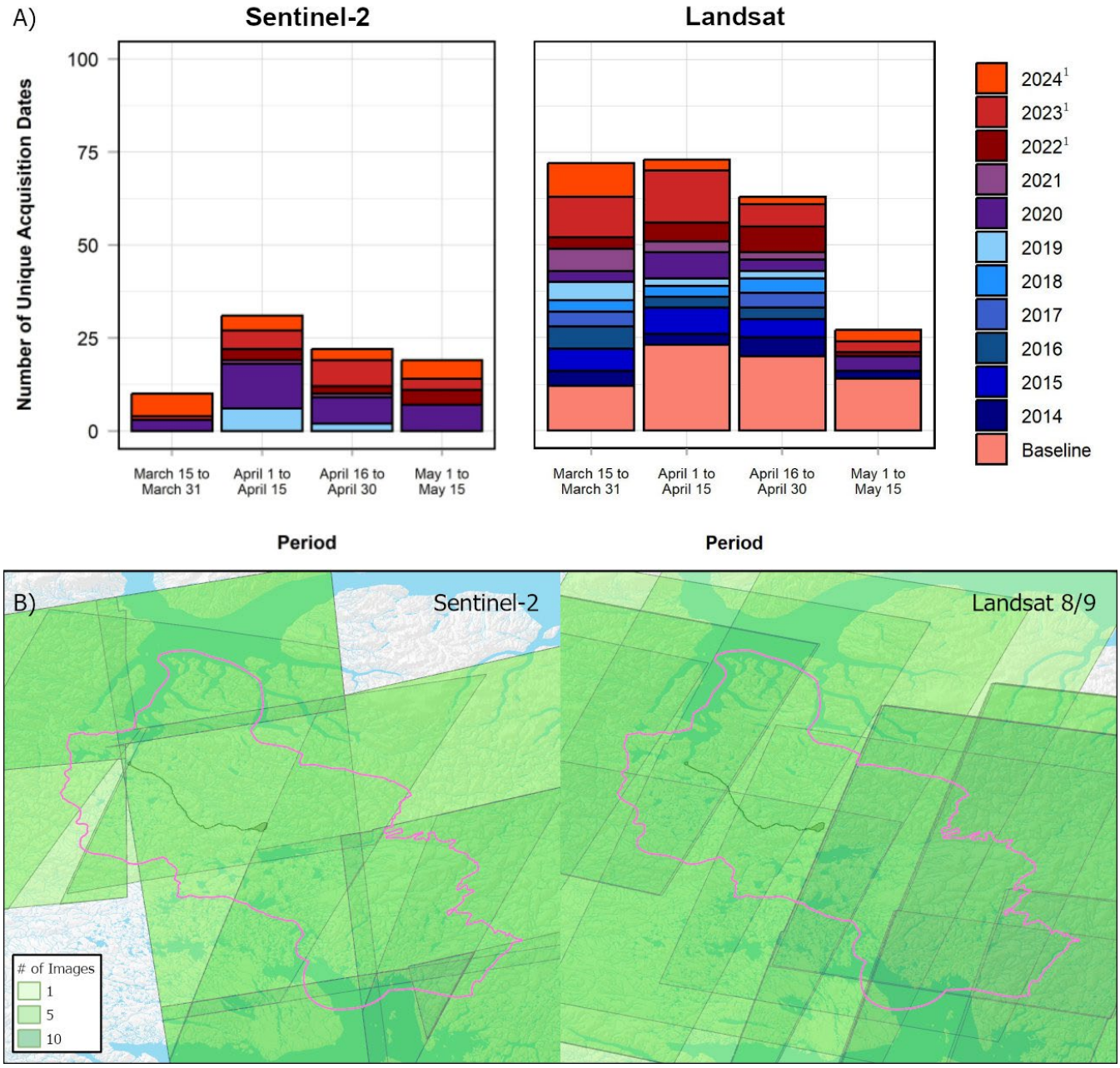

Figure 7-14. A) Sentinel-2 and Landsat unique acquisition dates per year for dustfall imagery analysis (March 15 to May 15) and B) the spatial coverage of the 2024 imagery.

1 Landsat imagery included Landsat 8 and 9 data.

7.4.2.2 Dustfall Concentration Estimation

The linear regression models used dustfall accumulation between the image acquisition date and the last snowfall event using the deposition rates from the passive dustfall monitoring sites. The 2021 data were excluded due to issues with the precipitation measurements. The relationship between the dustfall accumulation Df and the SDI values from Landsat imagery SDI_L is presented in Figure 7-15; the equation is provided below (F_{1308} = 144.5, P <0.0001, R^2 = 0.10).

$$SDI_L = 0.00140 \times Df + 0.00630$$

The relationship between the dustfall accumulation Df and the SDI values from Sentinel-2 imagery SDI_{S2} is presented in Figure 7-16; the equation is provided below (F_{331} = 141.8, P <0.0001, R^2 = 0.30).

$$SDI_{s2} = 0.00335 \times Df + 0.0166$$

The Sentinel-2 linear model had a higher R^2 value than the Landsat linear model but was limited to lower dustfall accumulation values. The weak relationships may indicate other factors involved, such as dust dispersion. However, the linear models can estimate dust concentration using the SDI values derived from satellite imagery to identify general spatial variability and temporal trends.

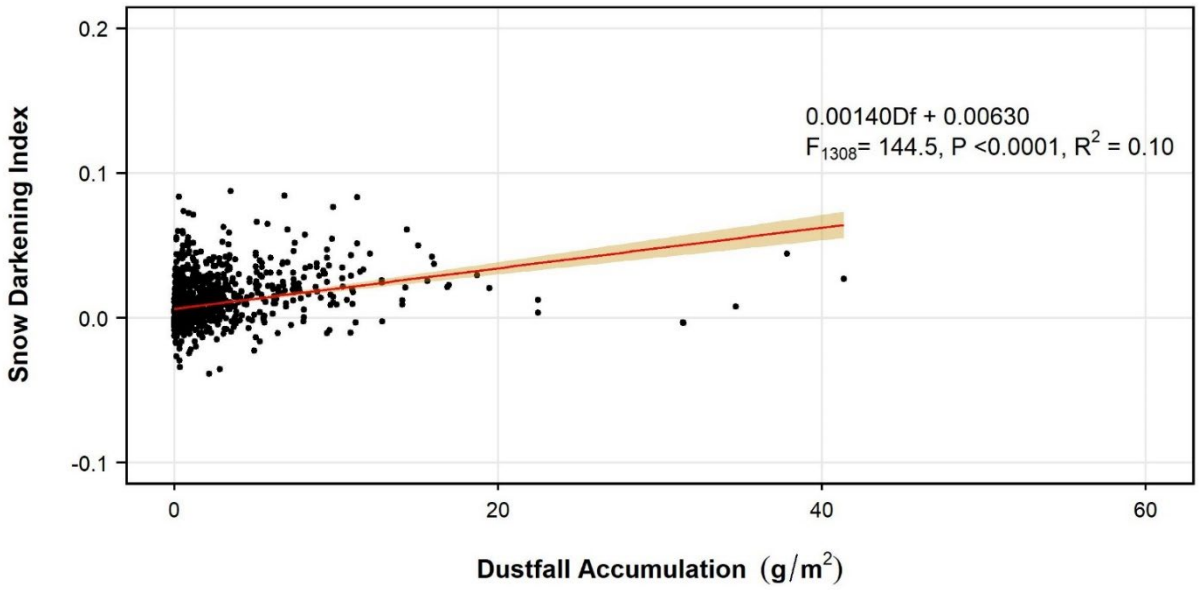

Figure 7-15. Relationship between calculated dustfall accumulation from passive dustfall deposition rates and Landsat 8/9 Snow Darkening Index.

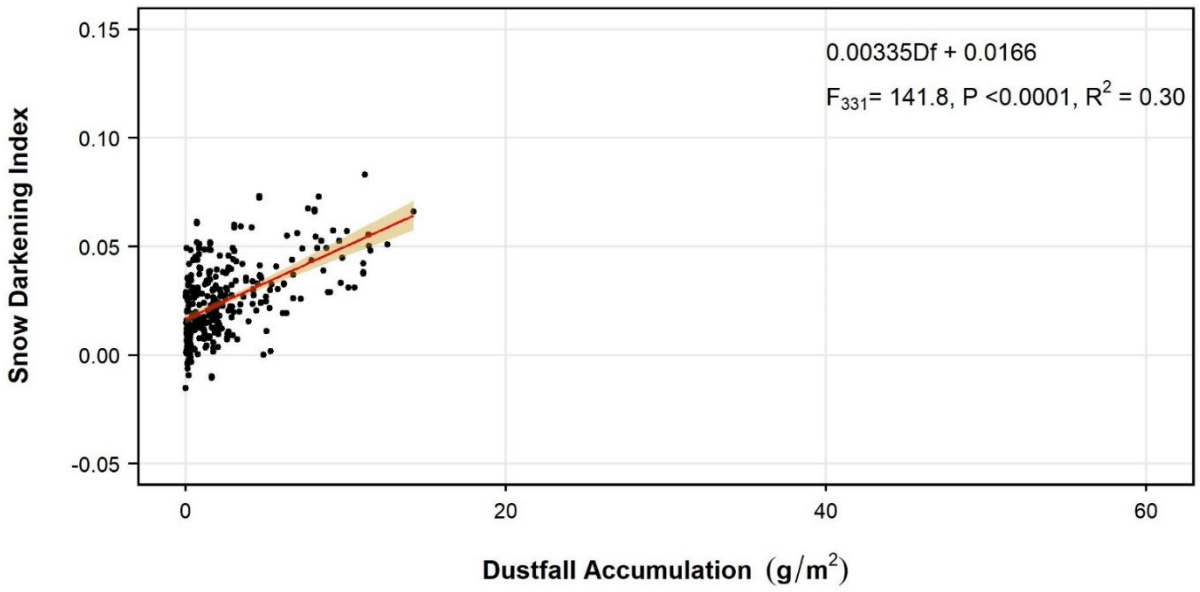

Figure 7-16. Relationship between calculated dustfall accumulation from passive dustfall deposition rates and Sentinel-2 Snow Darkening Index.

7.4.2.3 Magnitude and Extent of 2024 Dustfall

The 'extracted' dustfall extents and concentrations represent possible mineral dust accumulated on the snow cover. Dustfall extents and concentrations derived from Sentinel-2 and Landsat images were combined to reduce the effect of low image coverage from one satellite and to provide a more consistent dataset for inter-annual comparisons. Dust concentrations from remote sensing are estimates and represent the total dustfall accumulation over the satellite image capture period (i.e., mid-March to mid-May). These values are not equivalent to annual dustfall deposition.

Map 7-3 and Map 7-4 represent 2024 dustfall extents and concentrations above baseline values, where baseline values are the mean dustfall concentrations calculated between 2004 and 2013. Identification and contributions from dust sources cannot be determined solely from the satellite imagery analysis presented herein. Possible dust sources across the landscape include naturally exposed/unvegetated ground, wind-exposed ridges, and mining operations (e.g., stockpiles, road traffic, and mining). Trends in dustfall extent and concentration around Project infrastructure (e.g., Milne Port, Map 7-3 and Map 7-4) suggest that the primary source of dust is related to mining operations, as expected. In the outer surrounding terrain away from existing Project infrastructure, dustfall extents and concentrations likely occur and originate from multiple naturally occurring sources and/or are indicative of south-facing slopes and exposed bare ground as they were present in the baseline period.

The 2024 dustfall extent covered 12.71% of the Study Area (Table 7-8 and Figure 7-17). Dust concentrations of <1 g/m² and 1 to 4.5 g/m² accounted for the largest areas at 3.99% and 5.47%, respectively, followed by 4.5 to 10 g/m² at 2.16%. Areas with concentrations >10 g/m² accounted for 1.08% of the Study Area. The Tote Road south and Mine Site had the largest percentage of dust extent at 28.20% and 19.86%, respectively,

followed by Milne Port at 16.33%. The Tote Road north and Milne Inlet had the lowest percentage of dust extent at 9.64% and 6.93%, respectively. These values decreased from 2023 except for the Tote Road south area, but follow a similar pattern across the concentration classes.

Dustfall concentrations were highest at all sites within the PDA and decreased with distance from the Project (Figure 7-18), as reflected in the passive dustfall monitors (Section 7.3). The Milne Port area had the highest mean dustfall concentrations within the PDA, followed closely by the Tote Road south area. Outside of the PDA up to 30 m, Milne Inlet had the highest mean dustfall concentrations. The Tote Road north area had the lowest mean dustfall concentrations outside of the PDA.

Mine Site — Dustfall extended to the northwest and southwest, reflecting the predominant winds from the southeast to northeast and uncommon but strong easterly winds (Map 7-3 and Map 7-4; Section 4). Dustfall extended beyond the modelled TSP isopleths, primarily to the northwest. Dustfall extent was greatest for the 1 to 4.5 g/m² dustfall concentration class at 8.46% of the Mine Site area and decreased from 4.12% to 0.14% for concentration classes >4.5 g/m² (Table 7-8 and Figure 7-17). Mean dustfall concentrations decreased from 15.6 g/m² within the PDA to 1.1 g/m² within the 5 to 20 km buffer (Figure 7-18).

Milne Port — Around Milne Port (excluding Milne Inlet), dustfall extended to the north and southwest (Map 7-3). Dustfall extended beyond the modelled TSP isopleths in these directions. Dustfall extent mirrored the Mine Site with the greatest extent in the 1 to 4.5 g/m² (6.85%) dustfall concentration class, followed by a decrease in dustfall extent for concentration classes >4.5 g/m², dropping from 2.95% to 0.03% (Table 7-8 and Figure 7-17). Mean dustfall concentrations decreased from 26.7 g/m² within the PDA to 1.0 g/m² within the 5 to 20 km buffer (Figure 7-18).

Milne Inlet — Dustfall extended northeast along Milne Inlet, beyond the modelled TSP isopleths, most likely carried by strong southwest winds (Map 7-3 and Map 7-4; Section 4). Milne Inlet had the lowest percent area in concentration classes <4.5 g/m². Dustfall extent peaked at the 1 to 4.5 g/m² (2.29%) dustfall concentration class, followed by a decrease in dustfall extent for concentration classes >4.5 g/m², dropping from 1.18% to 0.00% (Table 7-8 and Figure 7-17). Mean dustfall concentrations decreased from 16.0 g/m² within the PDA to 0.0 g/m² within the 5 to 20 km buffer (Figure 7-18) but were higher further from the PDA (>30 m) than the other areas.

The Tote Road North — Dustfall extent along the road was within the modelled TSP isopleths. Dust was also present on the southern slopes of the terrain to the northeast (Map 7-3 and Map 7-4). Dustfall extent was greatest for the 1 to 4.5 g/m² dustfall concentration class at 3.93% and decreased to 0.01% with increasing concentration class (Table 7-8 and Figure 7-17). Mean dustfall concentrations decreased from 19.5 g/m² within the PDA to 0.8 g/m² within the 5 to 20 km buffer (Figure 7-18).

The Tote Road South — Dustfall extended past the modelled TSP isopleths to the north between the Mine Site and the south crossing of passive dustfall monitors (km 78), as well as to the southwest where the Tote Road turns northwest to Milne Port (Map 7-3 and Map 7-4). Dustfall extent for the Tote Road south area was the greatest by percent and also had the highest geometric mean daily dustfall rates from the dustfall monitors (Figure 7-1). Dustfall extent peaked at the 1 to 4.5 g/m² (12.75%) dustfall concentration class, followed by a

decrease in dustfall extent for concentration classes >4.5 g/m², dropping from 4.32% to 0.02% (Table 7-8 and Figure 7-17). Mean dustfall concentrations decreased from 22.7 g/m² within the PDA to 1.8 g/m² within the 5 to 20 km buffer (Figure 7-18).

Areas of Community Concern[11] — The Ridge West site had the highest mean dustfall concentration at 6.00 g/m², followed by the Eastern Channel site at 3.50 g/m² (Table 7-9, Map 7-5). The remaining locations had mean dustfall concentrations <0.5 g/m². The lakes had mean dustfall concentrations below 0.20 g/m², with maximum values between 50.25 and 19.44 g/m², generally along the shoreline. Inuktorfik Lake, to the southwest of the Mine Site, had the highest mean dustfall concentration of the lakes at 0.16 g/m².

[11] As informed by the QIA. Non-lake locations were digitized from Figure 11 in the 2021 Dust Investigation report (Hutchinson Environmental Sciences Ltd. 2022) at a scale of 1:750,000. Mapped locations are representative but hold some inherent variability.

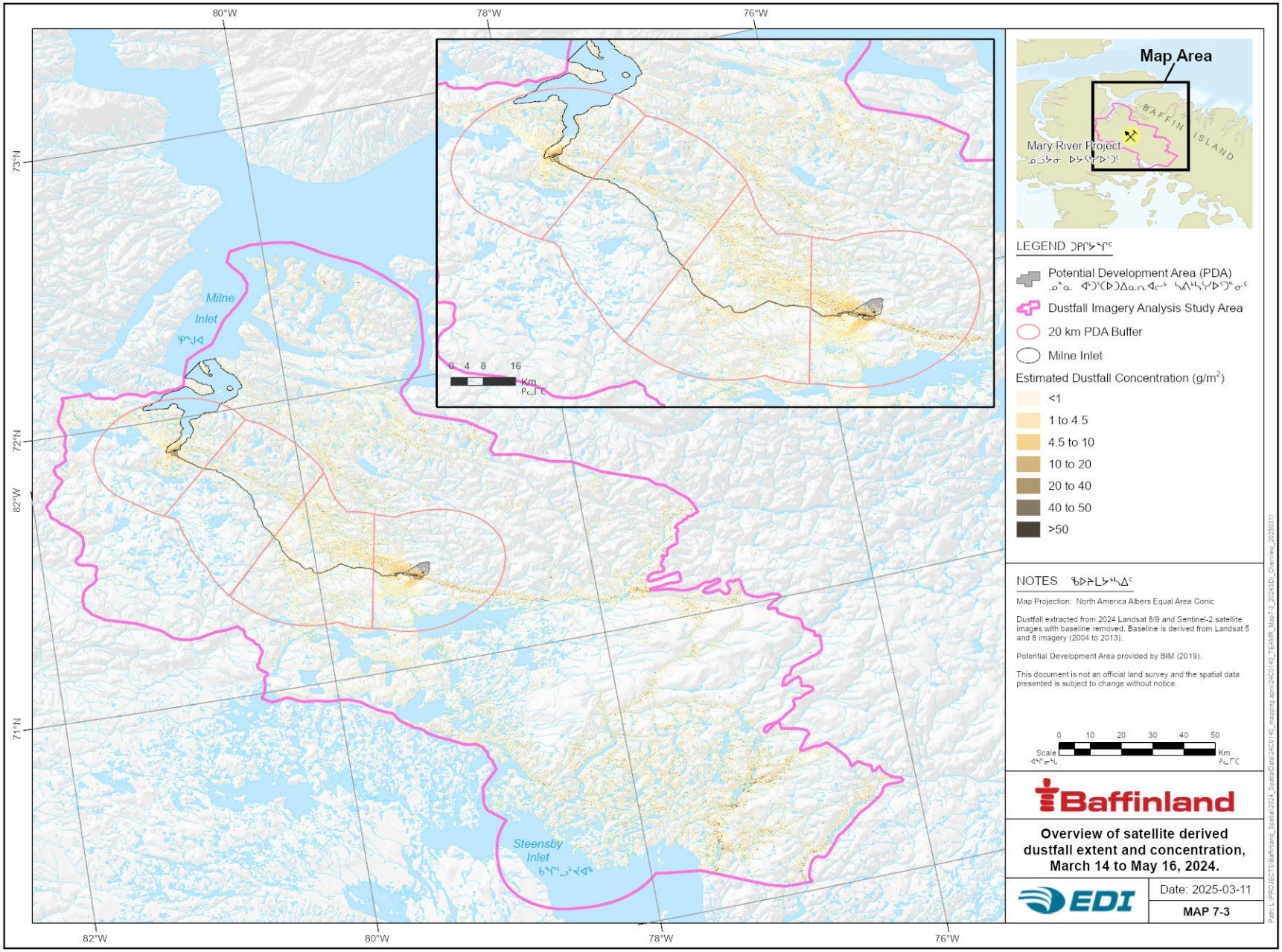
80°W
78°W
76°W
73°N
72°N
71°N
82°W
Milne Inlet
Steensby Inlet
0 4 8 16 Km
Map Area
Mary River Project
BAFFIN ISLAND
LEGEND
Potential Development Area (PDA)
Dustfall Imagery Analysis Study Area
20 km PDA Buffer
Milne Inlet
Estimated Dustfall Concentration (g/m²)
<1
1 to 4.5
4.5 to 10
10 to 20
20 to 40
40 to 50
>50
NOTES
Map Projection: North America Albers Equal Area Conic
Dustfall extracted from 2024 Landsat 8/9 and Sentinel-2 satellite images with baseline removed. Baseline is derived from Landsat 5 and 8 imagery (2004 to 2013).
Potential Development Area provided by BIM (2019).
This document is not an official land survey and the spatial data presented is subject to change without notice.
0 10 20 30 40 50 Km
Scale
Baffinland
Overview of satellite derived dustfall extent and concentration, March 14 to May 16, 2024.
EDI
Date: 2025-03-11
MAP 7-3

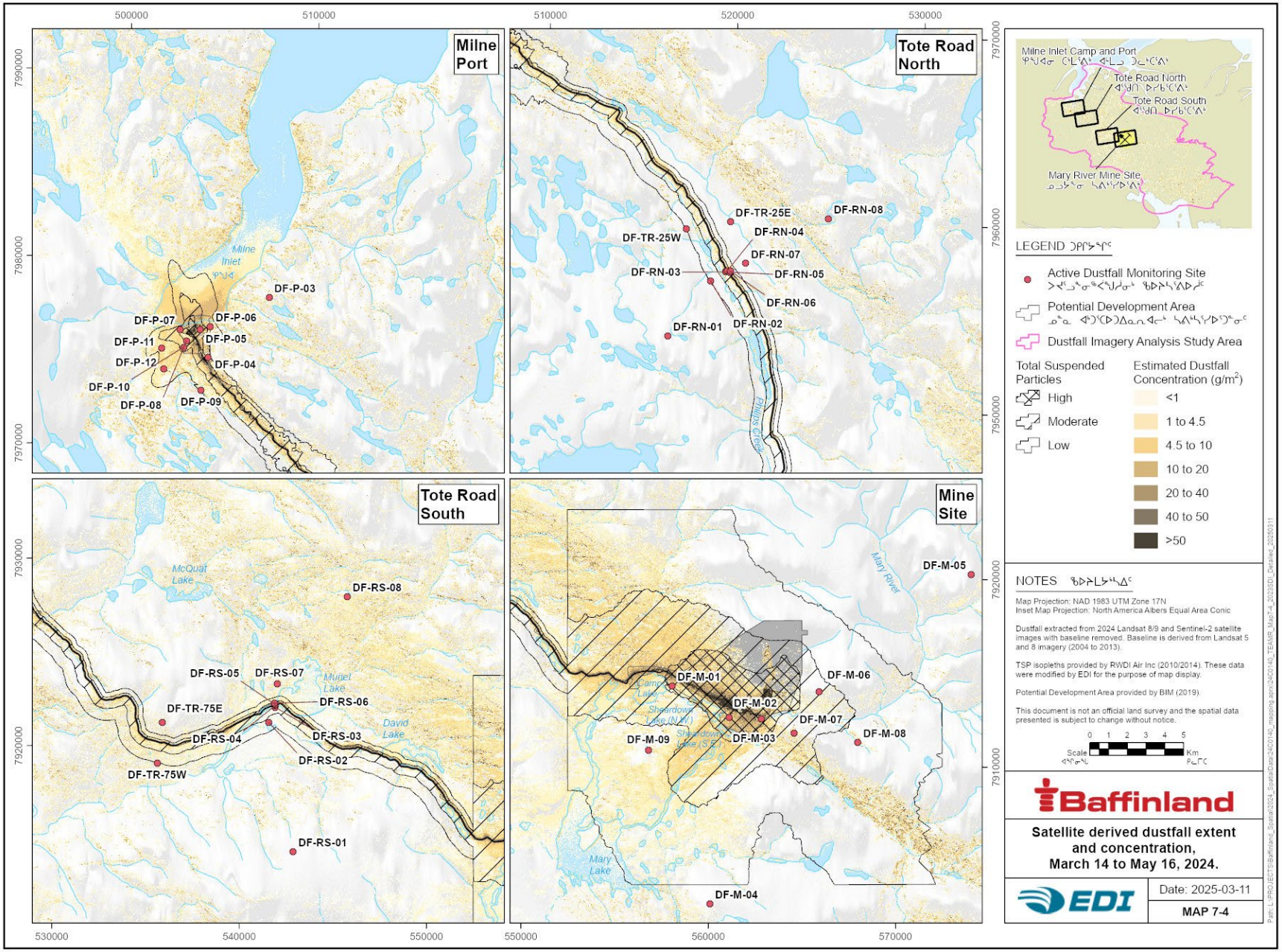
Milne Port
Tote Road North
Tote Road South
Mine Site
DF-P-03
DF-P-04
DF-P-05
DF-P-06
DF-P-07
DF-P-08
DF-P-09
DF-P-10
DF-P-11
DF-P-12
DF-TR-25E
DF-TR-25W
DF-RN-01
DF-RN-02
DF-RN-03
DF-RN-04
DF-RN-05
DF-RN-06
DF-RN-07
DF-RN-08
DF-RS-01
DF-RS-02
DF-RS-03
DF-RS-04
DF-RS-05
DF-RS-06
DF-RS-07
DF-RS-08
DF-TR-75E
DF-TR-75W
DF-M-01
DF-M-02
DF-M-03
DF-M-04
DF-M-05
DF-M-06
DF-M-07
DF-M-08
DF-M-09
Milne Inlet
McQuat Lake
Muriel Lake
David Lake
Mary River
Mary Lake
Camp Lake
Shoredown Lake (N.L.)
Shoredown Lake (S.L.)
Milne Inlet Camp and Port
Tote Road North
Tote Road South
Mary River Mine Site
LEGEND
Active Dustfall Monitoring Site
Potential Development Area
Dustfall Imagery Analysis Study Area
Total Suspended Particles
High
Moderate
Low
Estimated Dustfall Concentration (g/m²)
<1
1 to 4.5
4.5 to 10
10 to 20
20 to 40
40 to 50
>50
NOTES
Map Projection: NAD 1983 UTM Zone 17N
Inset Map Projection: North America Albers Equal Area Conic
Dustfall extracted from 2024 Landsat 8/9 and Sentinel-2 satellite images with baseline removed. Baseline is derived from Landsat 5 and 8 imagery (2004 to 2013).
TSP isopleths provided by RWDI Air Inc (2010/2014). These data were modified by EDI for the purpose of map display.
Potential Development Area provided by BIM (2019).
This document is not an official land survey and the spatial data presented is subject to change without notice.
Scale
Km
Baffinland
Satellite derived dustfall extent and concentration, March 14 to May 16, 2024.
EDI
Date: 2025-03-11
MAP 7-4

Table 7-8. 2024 dustfall area extent (km² and %) by concentration classes derived from Landsat and Sentinel-2 imagery.

Concentration Class	Units	Study Area	Mine Site	Milne Port	Milne Inlet	Tote Road South	Tote Road North
<1 g/m²	km²	1072.10	70.81	52.21	5.35	134.32	47.95
	%	3.99	5.09	5.13	1.91	9.47	3.31
1 to 4.5 g/m²	km²	1470.46	117.62	69.73	6.40	180.87	56.96
	%	5.47	8.46	6.85	2.29	12.75	3.93
4.5 to 10 g/m²	km²	581.96	57.25	30.01	5.07	61.22	22.26
	%	2.16	4.12	2.95	1.81	4.32	1.54
10 to 20 g/m²	km²	221.01	20.21	10.90	2.44	18.64	9.24
	%	0.82	1.45	1.07	0.87	1.31	0.64
20 to 40 g/m²	km²	59.27	7.24	2.69	0.11	4.30	2.74
	%	0.22	0.52	0.26	0.04	0.30	0.19
40 to 50 g/m²	km²	5.55	1.14	0.28	0.01	0.40	0.26
	%	0.02	0.08	0.03	0.00	0.03	0.02
>50 g/m²	km²	5.56	1.92	0.34	0.01	0.35	0.12
	%	0.02	0.14	0.03	0.00	0.02	0.01
Total Extent	**km²**	**3415.91**	**276.19**	**166.16**	**19.39**	**400.10**	**139.53**
	%	**12.71**	**19.86**	**16.33**	**6.93**	**28.20**	**9.64**

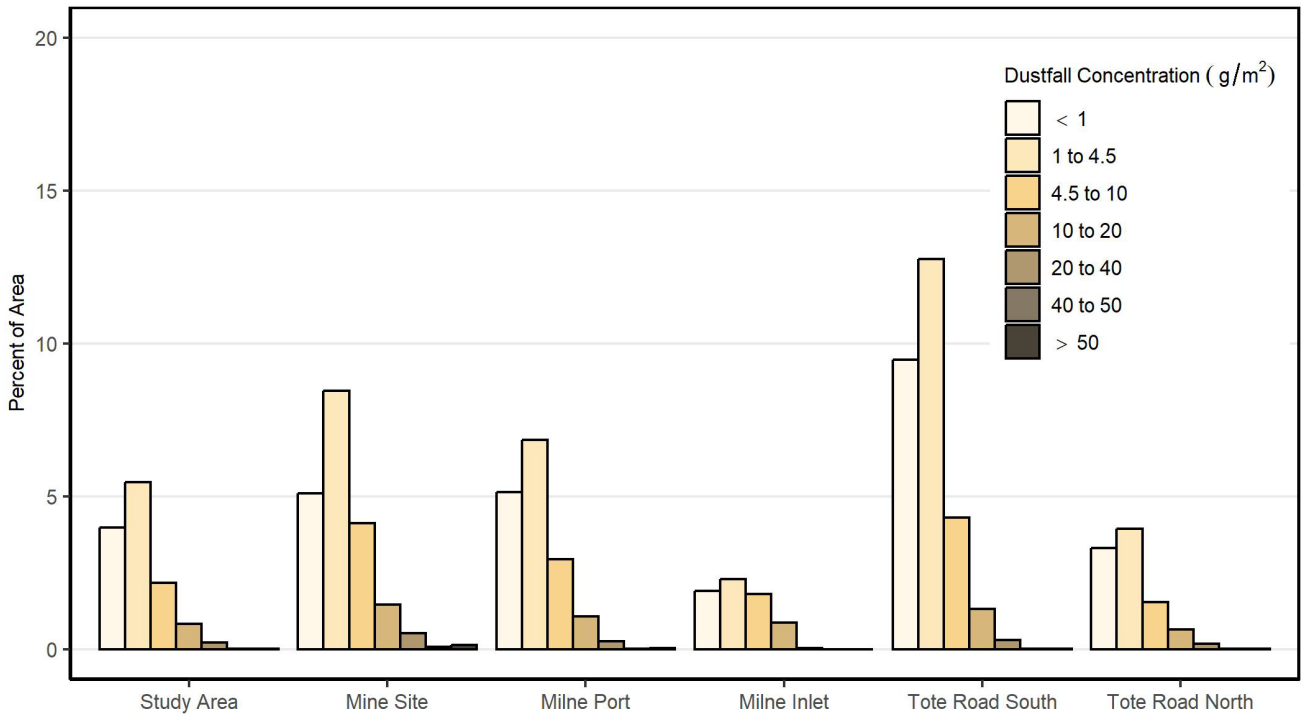

Figure 7-17. Percent dustfall area by concentration class within the Study Area for 2024.
The mean baseline has been removed from the data.

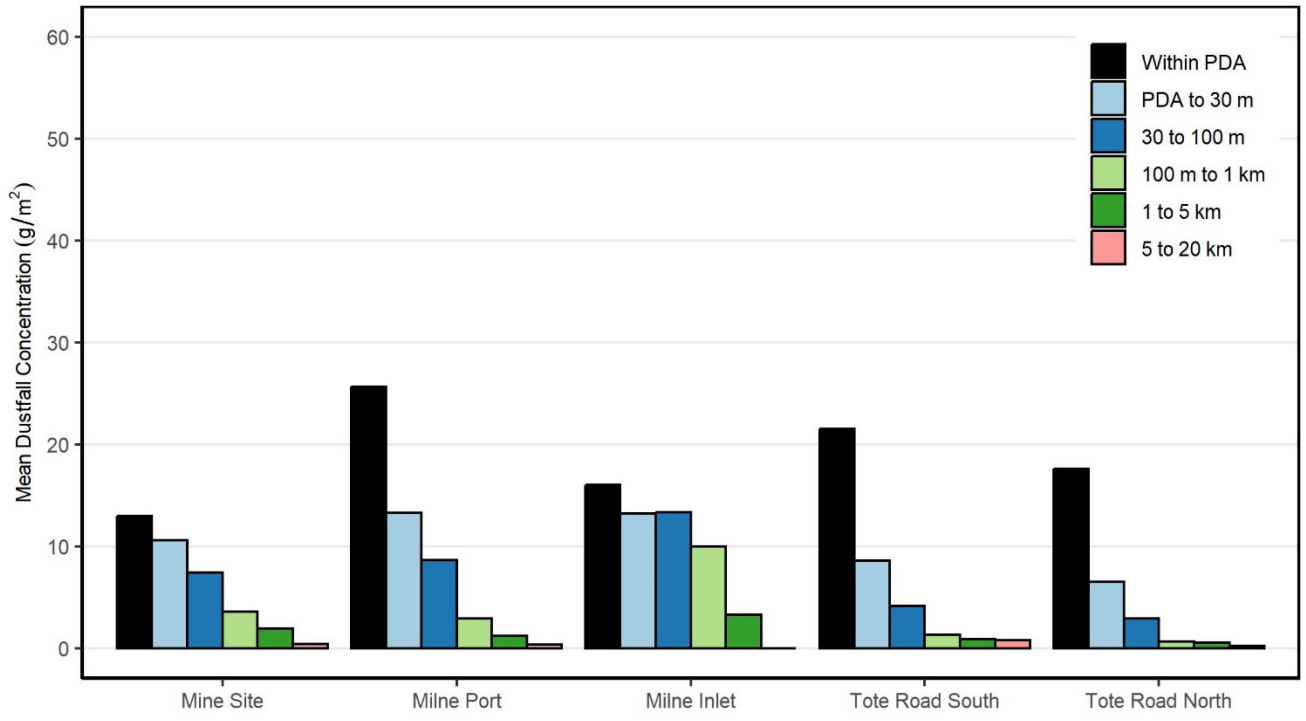

Figure 7-18. Mean dustfall concentrations within the Potential Development Area and 30 m, 100 m, 1 km, 5 km, and 20 km buffers for 2024.
The mean baseline has been removed from the data.

Table 7-9. Estimated 2024 mean, minimum, and maximum dustfall concentrations in Areas of Community Concern.

Location	Mean Dustfall Concentration (g/m²)	Standard Deviation (g/m²)	Minimum Dustfall Concentration (g/m²)	Maximum Dustfall Concentration (g/m²)
Pamiujaq	0.00	0.00	0.00	0.00
Eastern Channel	3.50	3.05	0.00	8.52
Mouth of Tugaat	0.00	0.00	0.00	0.00
Quarnak	0.13	0.47	0.00	2.21
Mine Site 40 WNW	0.50	1.72	0.00	8.20
Kanajjuk	0.00	0.00	0.00	0.00
Ridge West	6.00	4.73	0.00	15.88
Qullutu Lake	0.04	0.45	0.00	19.44
Angajurjualuk Lake	0.08	0.74	0.00	26.53
Inuktorfik Lake	0.16	1.04	0.00	50.25
Reference	0.00	0.00	0.00	0.00

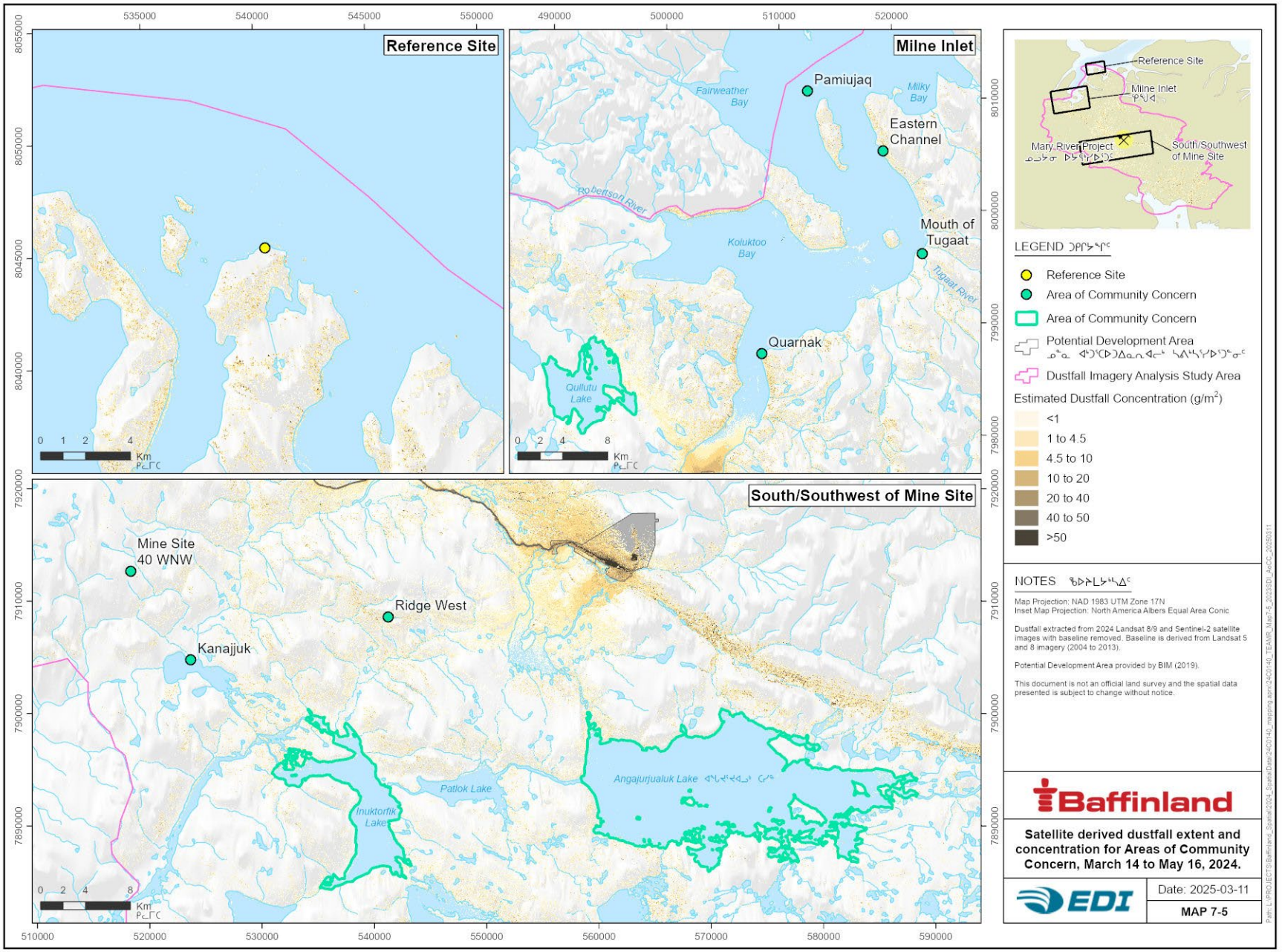
Reference Site
Milne Inlet
South/Southwest of Mine Site
Pamiujaq
Eastern Channel
Mouth of Tugaat
Quarnak
Fairweather Bay
Milky Bay
Robertson River
Koluktoo Bay
Tugaat River
Quilutu Lake
Mine Site 40 WNW
Ridge West
Kanajjuk
Patlok Lake
Inuktorfik Lake
Angajurjualuk Lake
Mary River Project
South/Southwest of Mine Site
LEGEND
Reference Site
Area of Community Concern
Area of Community Concern
Potential Development Area
Dustfall Imagery Analysis Study Area
Estimated Dustfall Concentration (g/m²)
<1
1 to 4.5
4.5 to 10
10 to 20
20 to 40
40 to 50
>50
NOTES
Map Projection: NAD 1983 UTM Zone 17N
Inset Map Projection: North America Albers Equal Area Conic
Dustfall extracted from 2024 Landsat 8/9 and Sentinel-2 satellite images with baseline removed. Baseline is derived from Landsat 5 and 8 imagery (2004 to 2013).
Potential Development Area provided by BIM (2019).
This document is not an official land survey and the spatial data presented is subject to change without notice.
Baffinland
Satellite derived dustfall extent and concentration for Areas of Community Concern, March 14 to May 16, 2024.
EDI
Date: 2025-03-11
MAP 7-5

7.4.3 INTER-ANNUAL TRENDS

Dustfall extents across all areas had a small peak in 2014/2015 followed by a larger peak in 2019, primarily in the <4.5 g/m² dustfall concentration classes (Figure 7-19). A visual review of the 2019 images showed less snow cover than images in the same year with less extensive dust and images in 2020 around the same dates. Baffin Island experienced lower than normal snow depths and early snow melt in 2019 (Richter-Menge et al. 2019), which may contribute to the reduced snow cover in the images. Less snow cover could result in more exposed ground, a possible source of dust, and potential misclassification of ground as dust. No peaks in total annual ore hauled or Tote Road traffic in 2019 compared to 2018 and 2020 (Figure 6-1).

The 2024 Study Area dustfall extent was comparable to 2023, with an increase in extent in the Tote Road south area, balanced by decreases in the other areas. The post-baseline years before 2018 and 2021/2022 in some areas (e.g., the Tote Road) had overall dustfall extents similar to or lower than the 2004 baseline year, but larger extents in the higher dustfall concentration classes (>20 g/m²).

The pattern of dustfall extent on the landscape was similar from 2014 to 2024 for all areas, with the highest concentrations near the Project and dustfall extending northeast along Milne Inlet, west and south of the Mine Site, and southwest of the Tote Road south crossing (km 78) in the direction of prevailing and/or strong winds (Map 7-6 to Map 7-13). Extensive dust occurred across all areas in 2019.

Satellite-derived mean dustfall concentrations across all areas generally increased from 2014 to 2020 in line with increased ore production (Figure 7-20 and Figure 7-15, Section 7.3). The mean dustfall concentration decreased in 2021. All areas showed increased mean dustfall concentrations in 2022 and 2023, followed by a decrease in 2024. The dustfall monitor data also observed a decrease in daily dustfall rates in 2024 compared to previous years (Section 7.3.3.1).

The overall trends between the satellite-derived late winter mean dustfall concentrations and the annual dustfall from the passive dustfall monitors were similar for the Tote Road and Mine Site, capturing most of the same fluctuations, but the trends were different for Milne Port (Figure 7-13).

Areas of Community Concern — The Reference site mean dustfall concentrations remained <1 g/m² for all years, with peaks at ~0.8 g/m² in 2018 and 2022. Most Areas of Community Concern also had mean dustfall concentrations <1 g/m² for all years (Pamiujaqa and Mine Site 40 WNW) or all years except for 2019 (Mouth of Tugaat, Qullutu Lake, Kanajjuk, Inuktorfik Lake, and Angajurjualuk Lake; Table 7-10 and Table 7-11). The mean dustfall concentrations at the Eastern Channel and Ridge West sites went over <1 g/m² more frequently (5 and 4 years, respectively), with one time during the 2004 baseline year. The Quarnak site, which generally falls within the dustfall extent from Milne Port out along Milne Inlet, reached mean dustfall concentrations of over 4 g/m² in 2018 and 2019.